April 2018

Sailbot 2017-2018

Travis Norris
Worcester Polytechnic Institute

Worcester Polytechnic Institute

Robotics Engineering Program

Sailbot 2017-2018 Final Report

A Major Qualifying Project Report
submitted to the Faculty of
WORCESTER POLYTECHNIC INSTITUTE
in partial fulfillment of the requirements for the
Degree of Bachelor of Science by:

Jordan Burklund, RBE/CS
Hans Johnson, RBE/ME
Travis Norris, RBE/PW
Liam Shanahan, ME

Project Advisors:
Professor Kenneth Stafford
Professor William Michalson

Date: 4/26/2018

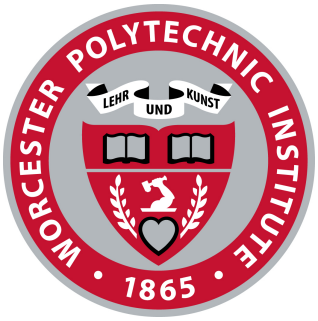

Abstract

The goal of this MQP was to build and program a robot capable of competing in the 2018 International Robotic Sailing Competition (IRSC), also known as Sailbot. This project utilized existing research on control and design of autonomous sailboats, and built on lessons learned from the last two years of WPI's Sailbot entries. The final product of this MQP was a more reliable, easier to control, and more innovative design than last year's event-winning boat.

Table of Contents

List of Figures

List of Tables

Acknowledgements

The 2017-18 Sailbot team would like to thank a number of people and companies who contributed to the success of this project. The WPI Robotics Club provided funding and assistance with the construction of the rigid wing sail, HydroCutter (Oxford, MA) donated waterjet services, Peterson Steel (Worcester, MA) donated aluminum stock, and both Howard Products (Worcester, MA) and DLC Manufacturing & Fabrication (New Ulm, MN) donated laser cutting services and material. We would also like to recognize Taylor North of Dimensional Polyant for donating sailcloth and connecting us to Chris Williams at Quantum Sails who helped design and cut the new cloth sail. Finally, we would like to thank our advisors, Professor Stafford and Professor Michalson for their input and guidance throughout the course of this project.

1 Introduction

The goal of this MQP was to build and program a robot capable of competing in the 2018 International Robotic Sailing Competition (IRSC), also known as Sailbot. Challenges in this competition include a fleet race, station keeping, navigation, payload transportation, collision avoidance, search, and endurance. This project utilized existing research on control and design of autonomous sailboats, and built on lessons learned from the last two years of WPI's Sailbot entries. The final product of this MQP was a more reliable, easier to control, and more innovative design than last year's event-winning boat. We utilized similar construction techniques, such as fiberglassing, laser cutting, and marine waterproofing. The boat was designed to sail primarily with a rigid wing sail developed by a previous MQP project. A new hull design and the inclusion of a functional movable ballast system was complimented by a redesigned NMEA 2000 compatible motor controller, and a vision system to significantly improve the boat's ability to round buoys when sailing a prescribed course. While entry into the International Robotic Sailing Competition (IRSC) was outside the scope of this MQP, the challenges and rules of that competition were used to constrain our design envelope and guide design features.

2 Background

2.1 – International Robotic Sailing Competition (IRSC)

The IRSC, formerly known as the International Robotic Sailing Regatta (IRSR), is an annual robotics competition where university teams compete to build unmanned sailboats to perform a variety of challenges with little-to-no human interaction. The Sailbot division involves boats of up to two meters in length, competing in challenges including racing, station keeping, obstacle avoidance, search, and endurance. The 2018 competition will be hosted by Worcester Polytechnic Institute in June, 2018.

2.2 – IRSC Robot Rules

The rules for the IRSC as of June 2014 are as follows [18]:

1. Overall length including hull, all spars and foils oriented in their fore and aft directions and at their maximum extensions if applicable, shall not exceed 2 meters measured parallel to the waterline. Sensors and their mountings are not included in the overall length measurement. Floating waterline must be clearly marked for use during measurement.
2. Beam shall not exceed 3 meters overall width at zero heel angle.
3. Number of hulls, depth, mast height, number of masts, sail area, and number of sails are unrestricted subject to the following event limitations:
   (a) The draft in normal sailing condition shall not exceed 1.5 meters.
   (b) Total overall height from the lowest underwater point to the highest point on the largest rig shall not exceed 5 meters. Sensors and their mountings are not included in the height measurement.
4. Teams shall provide a suitable stand to support the boat in a vertical position while fully assembled for the purposes of judging.
5. Boats shall not have any direct human contact during on-the-water events except as permitted by the event Notice of Competition and Sailing Instructions
6. External control shall be limited as specified in the event Notice of Competition and Sailing Instructions, however a means for full remote radio control is required at all times during competition to allow avoidance of collisions with other boats.
7. Data transfer from the boat to shore is unlimited, but shall be on an approved frequency.
8. Radio frequencies used by each boat shall comply with host country regulations and are subject to approval before competition.
9. In each event, boats shall compete by sailing only (no alternate sources of propulsion).
10. Construction materials are not restricted provided they cannot cause environmental damage during operation. In particular, lead ballast must be completely sealed.
11. Power for onboard control systems may be provided by any source other than biological, and must be fully contained within the vessel.
12. The configuration of the boat shall not change during the course of any event. (i.e. components cannot be jettisoned or added during the race). Bilge pumps are permitted as long as they do not provide additional propulsion to the vessel.
13. Any parts may be replaced or repaired between events as necessary.
14. Sail configuration changes (hoisting/dousing) are allowed during a race provided such a change is initiated and executed only by the onboard systems.
15. In case of uncertainty about interpretation of these rules, please contact the event organizers for clarification.

2.3 – IRSC Challenges

The IRSC consists of seven challenges: Fleet Race, Station Keeping, Navigation, Payload, Collision Avoidance, Search, and Endurance. The following section briefly describes each event.

Fleet Race
All boats compete simultaneously to sail a triangular course. Steering is done by remote control, but sail control may be autonomous.

Station Keeping
The boat must autonomously enter and stay within 40 x 40 meter box for five minutes, and autonomously exit within one minute.

Navigation
The boat must autonomously sail a triangular course with 50 meter legs, and return between the two starting buoys.

Payload
The boat must sail a 100 meter course and return while carrying a weighted payload.

Collision Avoidance
The boat will sail a 100 meter course and return. During the trip, a separate boat will approach on a collision course. The boat must autonomously respond and avoid the approaching boat.

Search
The boat must execute a search pattern to locate and touch an orange buoy, randomly placed within 100 meters of the start position.

Endurance
The boat will sail a rectangular course for up to 8 hours.

2.4 – Robotic Sailing

To design fully autonomous sailboats, researchers have proposed several hardware and software designs. Plumet et al. [33] describe the architecture for a prototype autonomous sailboat. To navigate, the Autonomous SAiling Robot for Oceanographic MEasurements (ASAROME) platform uses wind speed, GPS, and IMU sensors, and controls its movement with actuators on the boom and rudder. To detect surrounding obstacles, the ASAROME project uses a combination of a panoramic camera, sonar, and two hydrophones. The camera detects objects above the surface, while the sonar and hydrophones detect submerged obstacles. In addition, the authors propose a potential-field path-planning model based on obstacles, wind speed, and potential for tacking. Previous research has also examined control theory for robotic sailboats. Sauod et al. [37] examine a 3-DOF dynamics controller for managing the x position, y position, and heading of an autonomous sailboat using rudder control and sail trim. The controller optimizes sail trim to provide maximum lifting force, and navigates based on a course (velocity vector), rather than a desired heading. Additionally, the researchers created a switching controller that acts as a heading controller at low speed, and a course controller at higher speeds. This controller proved to be the best for navigation because it reduces the effects of noise at low speeds, and provides the benefits of course control at high speeds. One drawback of this controller is that it does not maximize the sail trim for speed, but only for force.

2.5 – Previous Sailbots

2.5.1 – Mechanical Systems

WPI's two previous Sailbots (built in the 2015-16 and 2016-17 academic years) provided hands-on experience with the challenges involved in building and controlling autonomous aquatic vehicles. Prior to this year,

WPI's Sailbot teams derived their boats from existing hull shapes. In 2015-16, this was a one meter RC boat that was refitted with a custom control system. Last year, the team used a hull form donated by the U.S. Naval Academy as the starting point for fabricating a fiberglass hull, plywood internal structure, and fiberglass and plywood deck. Both previous boats suffered from water intrusion issues, limiting the maximum runtime of the boat and shortening the lifespan of electrical components. Both boats used similar style winches, with the mainsheet (and for the first boat, a jib sheet) passing through a fairlead into the hull where it wrapped around a motorized drum. When the mainsheet was slack, and the sails were sheeted out and then back in, the slack would often tangle around the winch, and require manual intervention to return the boat to service. The rudder design on both boats was also similar, with a servo actuating a single rudder through a four-bar linkage. Mechanically, this was an effective design on both boats; however the rudders lost authority when the boat heeled, making it more difficult to sail close to the wind.

2.5.2 – Boat Balance

Because the 2015-16 boat was purchased off the shelf, it was reasonably well balanced and relatively easy to control. The 2016-17 boat was designed to sail with an autonomous rigid wing sail developed by another MQP group, and the mast was located to be balanced using that sail. However, the wing sail was not reliable enough to use in the competition, and the team used the backup cloth sail instead. The center of effort of the cloth sail is further aft than the wing sail, causing an imbalance in the boat. This required the addition of a jib, which allowed the boat to complete a tack and sail efficiently upwind. The keel on last year's boat was donated by USNA, composed of a high aspect ratio stainless steel centerboard and a 27lb lead bulb. The short chord resulted in low lift at low speed, which necessitated the addition of a low aspect ratio wing just under the boat. This additional wing, constructed to be neutrally buoyant, significantly improved the low speed performance of the boat.

2.5.3 – Controls

The control systems for previous Sailbots have become more sophisticated as the projects have progressed. The 2015-16 boat used a Beaglebone Black as the central processor, and used an Arduino connected over UART to interface with the sensors on the boat. The boat included a GPS, 9-axis IMU, and wind vane sensor. These were then used in a simplistic control algorithm that set a desired heading based on the current and goal locations, and avoided headings that were too far up-wind. A servo controlled the rudder to direct the boat to the desired heading, and a multi-turn servo controlled the winch to optimize the sail position for the current relative wind.

The 2016-17 boat used more sophisticated sensors, algorithms, and control structure. The boat used an Airmar 220WX WeatherStation that reported GPS location, absolute wind speed and direction, relative wind speed and direction, current heading, and current heel angle on a NMEA 2000 bus. For detecting buoys and obstacles, the boat used a Raspberry Pi Zero with a camera, and used OpenCV with basic hue and saturation segmentation. Position of any buoys in the camera frame were then reported over a WiFi connection. A Beaglebone Black again acted as the central processor, using sensor information with a more sophisticated heading selection algorithm that considers the current state of the boat. Again, a servo-controlled rudder steered the boat to a desired heading. Because the sail area was larger with the 2016-17 boat, a custom winch was constructed with a window motor, and multi-turn potentiometer. To simplify electrical wiring, a custom interface board was designed to operate on the NMEA 2000 bus to send servo commands, and control the current winch position. With information about the current wind conditions, the winch control again optimized the sail position given the current state. The Beaglebone Black used a publish-scribe architecture to break the software processing components into several independent processes that communicated over a custom Inter-Process Communication (IPC) mechanism. This allowed the individual processes to be more flexible to changes in the architecture, and allow for identical software to run both in simulation and on the boat.

2.6 – Purpose

Robotic sailing has several real-world applications. Because they require no crew and little power, sailing robots can be used for long-term expeditions such as oceanic data collection [42] or coastal monitoring for

defense [26]. Additionally, sailing presents an interesting and challenging control problem with many areas of potential research.

The purpose of this project is to design and manufacture an autonomous sailboat that builds upon lessons learned from previous Sailbot projects. In this paper, we describe the mechanical, electrical, and software objectives for our project, and discuss the effectiveness of these designs. In particular, we describe the improvements to the hull, sails, rudder, and keel compared to last year's project. We also discuss the addition of a movable ballast system to control the heel of the boat. Next, we describe the design of the electrical system and the custom circuitry needed for this project. Third, we explain the software architecture and the controls of Sailbot, and the machine vision system used to detect nearby buoys. Finally, we detail the testing strategy and communication techniques used in this Sailbot project.

3 System Overview

For an autonomous sailboat to sail efficiently, the hardware and software must interface seamlessly. Sailing is a balancing act of forces and moments, which must be sensed, the proper response computed, and then acted upon using one of the boat's control surfaces. This year's boat has three degrees of freedom, which replicate a human sailor's tiller hand (rudder), sheet hand (winch or wing sail), and shifting weight (movable ballast). All of the systems designed this year work together to make the boat sail, with the electrical system providing sensor information to the software, the software determining the proper control outputs, and the mechanical system producing those outputs. These systems are tightly integrated, and designed to operate within the limits of other systems. These limits include the Angle of Attack (AoA) of the sail, the motion range of the rudders and movable ballast, and the current limits of the motor controllers.

3.1 – Mechanical Overview

The objective of a sailboat is to utilize wind power to travel in all directions in an efficient manner. While downwind travel is trivial, upwind travel depends on a few physical phenomena.

A sailboat consists of a few components, shown in Figure 1.

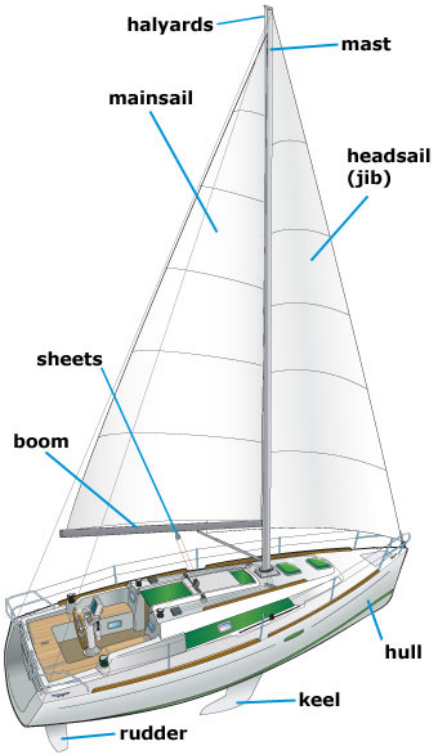

Figure 1: Parts of a Sailboat from [5]

The hull is often constructed from fiberglass and is designed to be streamlined to reduce drag in the water and stable to decrease the required righting moment to counter the force of the wind on the sails. The rudder is an underwater foil used to steer the boat to hold a course, or initiate a tack or gybe to change course. The sail is the above water lifting surface that produces the driving force for the vessel. The AoA or trim of the sail needs to be adjustable to optimize the lift for a given relative wind angle. A traditional sail is trimmed with a rope, called a mainsheet, that passes through pulleys to provide mechanical advantage. The primary below water lifting surface is called the daggerboard, or keel if it has attached ballast.

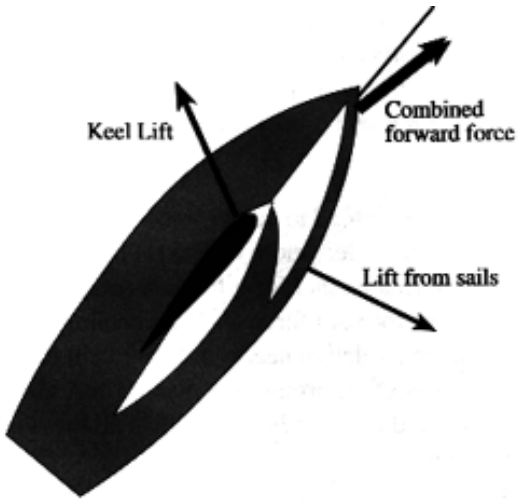

Figure 2: Forces on a Sailboat

The interaction between the sail and the lifting surface of the keel is the essential factor permitting a boat to sail upwind. In Figure 2, with wind flowing from top to bottom, the sail generates lift downwind while the keel generates an equal amount of lift upwind. The resultant of these two lift vectors propels the boat in a forward direction. Consequently, more efficient foils help the boat sail upwind more effectively, and optimizing upwind performance was a primary design parameter for this project.

All of the boat's mechanical systems were redesigned this year, using lessons learned from previous sailbots, good engineering practices, and a "build early, break early" mindset. Past WPI Sailbots suffered from water intrusion issues, limiting sailing time or requiring significant water absorption media (such as diapers) to prevent sloshing and protect electronics. Some of the sources of leaks that we identified on previous boats were hatches, the keel box, the rudder tubes, and the mainsheet fairlead. Waterproof marine hatches and proper use of fairing compound address the first two issues, maintaining a seal around the static components of the boat. The rudder tubes were redesigned to seal them through the hull and deck to prevent ingress of water via the rudders and the new winch design addresses the mainsheet fairlead issue.

3.2 – Electrical Overview

The electrical system for this year's boat is heavily derived from the 2016-2017 Sailbot. As Figure 3 shows, the backbone of the boat's electrical system is a NMEA2000 bus. NMEA2000 is a marine standard that provides both power and communication to devices connected to the bus. The communication portion of the standard is a 250 kbps CAN (Controller Area Network) bus, which is a noise-resistant, multi-master communication standard commonly used in many types of vehicles. NMEA2000 also provides 12 volt power, simplifying the wiring for most devices, and specifies waterproof connectors that meet at least IP67 standards.

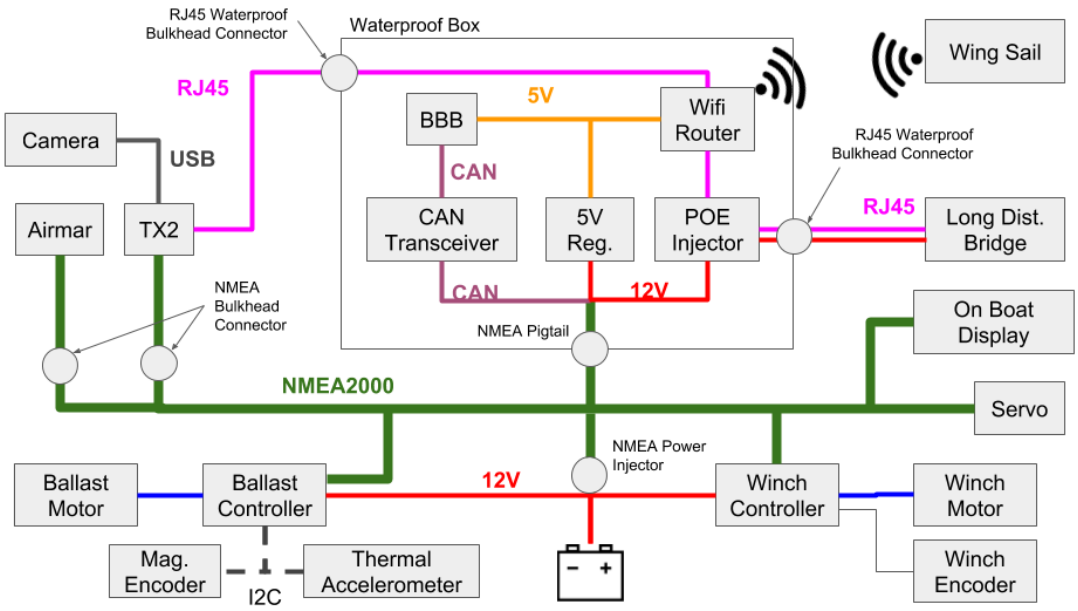

Figure 3: Electrical System Layout

NMEA2000 was selected over similar bus architectures (such as RS-485, LIN, and Ethernet) because the Airmar sensor unit used for wind direction and GPS already uses the NMEA2000 standard. Standard waterproof connectors and integrated power delivery supported this decision. The NMEA2000 based system proved to be simple, effective, and reliable for the 2016-17 boat, contributing to the decision to use it again this year as the basis for the boat communication network.

Ethernet provides the communication link for the boat to the outside world, linking the BeagleBone Black and NVIDIA TX2 to a WiFi router and the long-distance radio for software updates and transmitting boat telemetry information. WiFi provides high-bandwidth, relatively short range communication for data intensive tasks such as deploying code, while the long distance radios provide telemetry updates when the boat is operating outside of WiFi range.

3.3 – Software Overview

The overall software architecture is a continuation of the system developed by the 2017 Sailbot team [49]. The primary advancements made in this project focus on machine vision for obstacle detection and control of the movable ballast.

The BeagleBone Black software runs multiple processes which communicate using a publish/subscribe architecture (Figure 4), which shares messages between individual processes, or nodes. The Primary Control Node controls the path planning and overall decision making of the robot. The State Estimator Node provides the wind, heading, and position data, which is used to produce motor control outputs. The CAN Node communicates these outputs to the motor controllers on the CAN bus. Additional nodes are used for logging and debugging via a web interface.

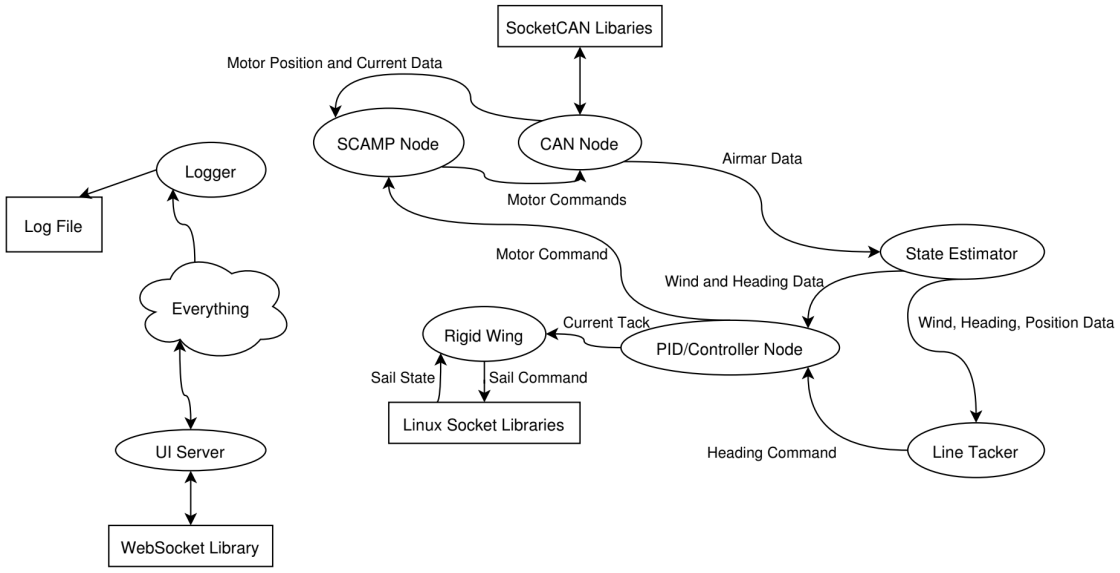

Figure 4: Node Structure and Communication from [49]

3.3.1 – Visual Buoy Identification

To identify buoys, the team tested several types of object detection using video footage collected from various sailing trips. The system needed to provide better estimates of where the buoys were located to navigate the course more accurately. A special colorspace transform was used to pre-filter noise, while convolutional filtering finds the buoy in a frame, and particle filtering estimates the location of the buoy.

3.3.2 – Movable Ballast Control

Controlling the movable ballast requires additions to the planning and control algorithms. The desired heel is calculated based on the relative wind direction. Additional sensors provide estimates of the heel and angle of the movable ballast at a frequency of 100 Hz. We tested several control options, and developed a method for controlling heel while limiting power consumption.

4 Design and Methodology

4.1 – Mechanical Components

4.1.1 – Hull

The design for this year's boat was motivated by experience with the previous hull form, donated by the US Naval Academy. The 2017 Sailbot hull had a narrow and deep displacement hull profile with a maximum beam of 30cm. While the narrow beam minimized canoe-body drag, it suffered from poor form stability and had limited internal volume for other boat components. While not a direct result of the hull design, the 2016-17 boat suffered from poor balance. Designing a hull with improved form stability, increased internal volume, and better balance was a key component of this year's project.

The geometry of the hull was designed with packaging, ballast, and sailing dynamics in mind. The bow and stern profiles of the hull were derived from modern, high performance open ocean sailing yachts such as the Imoca 60 and the Volvo 65 (Figure 5). These boat designs have proven to be light, stable, efficient, and seaworthy in all sailing conditions.

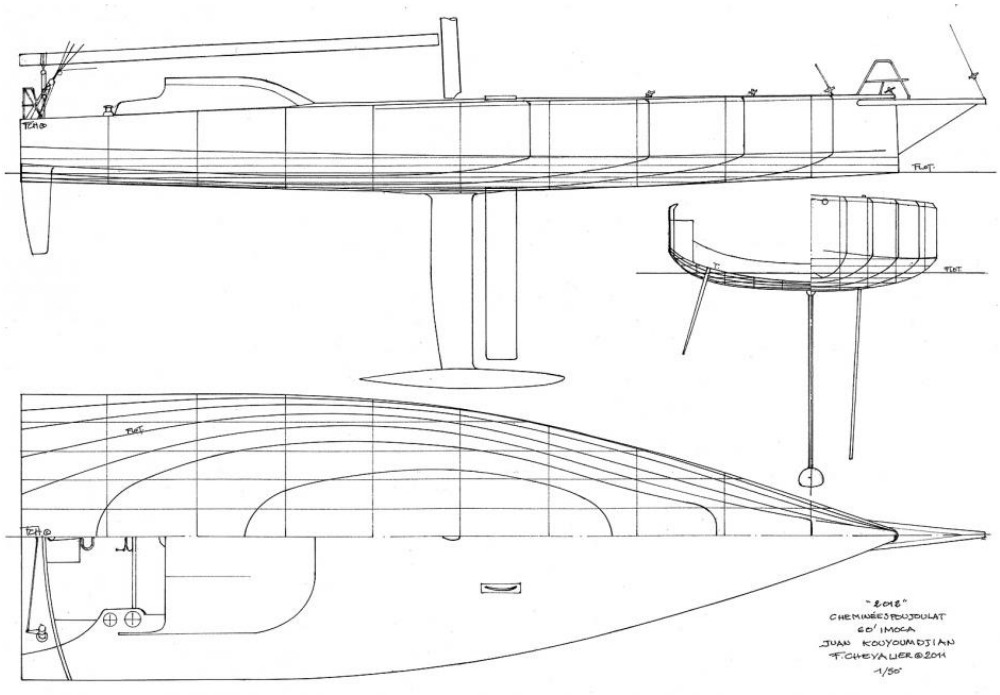

Figure 5: IMOCA 60 Line Plot

The features we replicated in our design include a wide 55 cm beam for good form stability, a shallow bottom for low water drag, a pointed nose for wave penetration, and a flat side profile to minimize hull steering due to induced heel.

Figure 6: Completed Hull

The wider stern and shallow draft of the new design increase buoyancy in the stern, which lifts the hull higher in the water and allows the boat to sail slightly faster than its theoretical hull speed due to the more gradual waterline wave. In addition, this flat bottom to steep edged stern design will decrease the wetted surface area when the boat is heeled, reducing skin drag. A comparison from the stern and top views below (Figures 7 and 8) illustrate the comparison between the hull profiles.

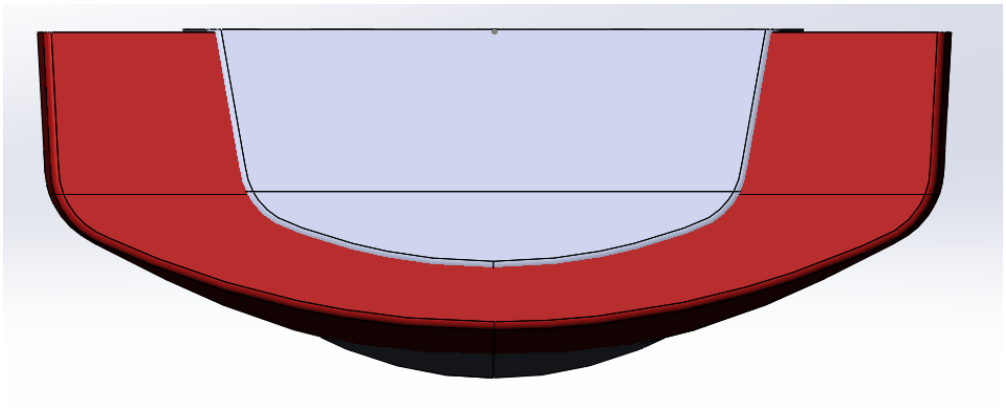

Figure 7: Comparison of Stern Profiles Between 2016-17 and 2017-18 Hulls

Figure 8 shows the top profile of the two hull designs. The narrow and elongated bow allows the boat to penetrate waves effectively, even with the wider maximum beam. The wider stern shifts the center of lateral resistance aft, allowing the sail to move further aft. Moving the sail aft drives the bow further out of the water and prevents diving under large waves.

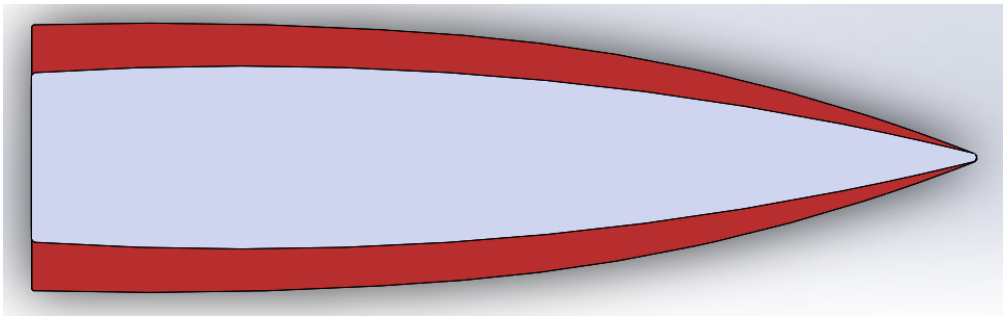

Figure 8: Comparison of Top Profiles Between 2016-17 and 2017-18 Hulls

CFD analysis was used to iterate the new hull design, and benchmark it against the previous hull design and a conventional "beamer" design. The stern flow simulations are shown in Figure 9, simulated at 20°of heel and a 5°angle of attack (aoa) through the water at 10 kts. By maintaining the max beam along the aft $\frac{1}{3}$ of the hull and maintaining a sharp transom edge, the hull ends its interface with the water abruptly and sheers from the water surface, minimizing stern drag. In contrast, the curvature of the previous displacement hull induced undesirable low pressure vortices at the transom.

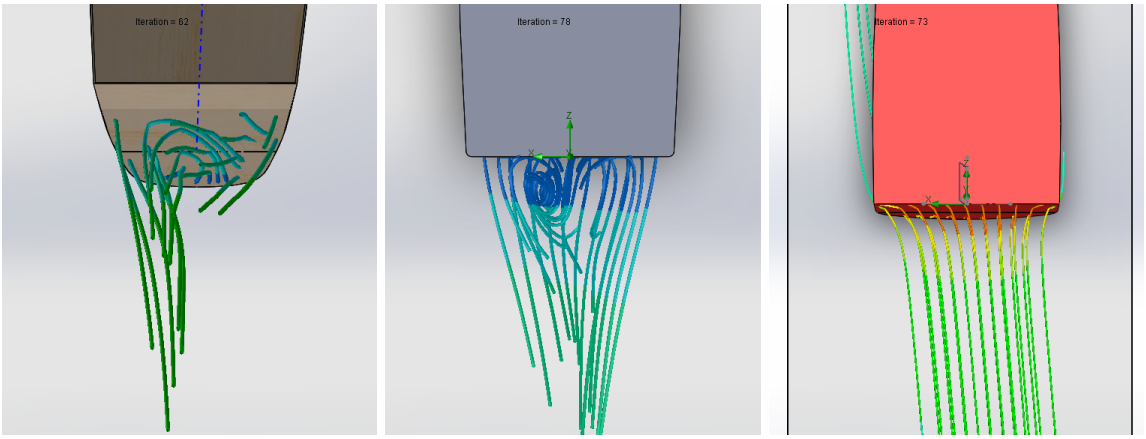

Figure 9: Comparison of Stern Flow Across Hull Designs

4.1.2 – Wingsail

A wingsail is a modern advancement in sailing technology that has been used in a number of high performance and experimental sailing vessels. In 2017 an MQP team designed and manufactured a wingsail for the 2017 Sailbot project. While the design concept showed promise, the weight of the final product induced excessive heel on the boat, and the control system was not robust enough for extended use. Testing showed that the wingsail made the more sailable in all wind conditions, justifying continued work on the project.

Figure 10: Wingsail Assembly

Because manufacturing was the limiting factor on the effectiveness of the previous wingsail, the decision was made to utilize theoretical and experimental data from the previous MQP team to incrementally improve the design, rather than redesigning the sail from scratch. The design constraints identified and imposed on the sail design were:

1. The wingsail must sail effectively on all points of sail under normal wind conditions (2-15kts).
2. The sail must have the ability to depower completely.
3. The sail must be self contained and wirelessly connected to the boat's control system.
4. Total height should not exceed 3.5m
5. The sail must be easily disassembled for transport.

To meet these constraints, the wingsail is free standing, free rotating, rigid, and has a symmetrical airfoil. To adjust the angle of attack of the sail, a trim tab controlled by a servo is mounted behind the trailing edge of the main sail area.

Design Changes

The primary goal of the wingsail redesign was to reduce weight. The 2017 sail weighed about 67 N and even in light air this weight induced significant heel on the boat, causing the boat to become unstable through tacks and gybes. The weight of this year's sail was reduced to 44 N, accomplished by replacing the thick fiberglass mast and aluminum trim tab rod with carbon fiber tubes, reducing the number of airfoil cross sections, and using balsa and foam to construct the cross sections rather than birch. The control system was relocated to an easily accessible compartment near the disassembly joint, and the counterbalance was relocated to the base of the sail, reducing the heeling moment that it provides. Enlarging the trim tab by 20% increased the lifting force that it provides to control the angle of attack of the sail, improving control of the sail at low wind speeds.

In the 2017 wing, poor mating of the cross sections to the trailing edge caused the end caps of the sail to flex under the compressive pressure of the Monokote skin. To counter this, thick foam end caps were used

at the top and bottom of the sail sections and a 3D printed trailing edge cap was fastened to hold the thin carbon fiber trailing edge in place.

The new mast selected for this year's wing sail was a 1.9 cm diameter woven carbon fiber tube, replacing the previous fiberglass RDM windsurfer mast. The carbon fiber mast is about 70% lighter, as well as more flexible. With a stiffness of 6 Nm^2 compared to the previous 96 Nm^2, the new mast is 5.8% the stiffness of the previous mast. To compensate for the increased flexibility, a tapered wooden dowel rod was inserted into the bottom 0.8 m of the mast. The dowel improves the crush strength of the carbon fiber at the stress concentrations where the mast rotates in the mast tube bushing, and where the mast enters the sail, as well as improving the overall stiffness.

Aerodynamic Analysis

Based on experimental data from the 2017 wing sail, we were able to validate and modify the design to fit the new boat dimensions and wind conditions.

A symmetrical airfoil is required for equal behavior for both positive and negative angles of attack, and the chord of the foil was limited by manufacturing constraints (a 60x45cm laser bed). The sail was designed in XFLR5 airfoil simulation software with an expected wind velocity based on historical data for Lake Quinsigamond, between 5 and 7 kts.

The foil section selected was a NACA 0183 section, as it provides the best performance through the expected wind speed range. The expected wind speed of 5 to 7 kts yields a Reynolds number range between 85,000 and 120,000.

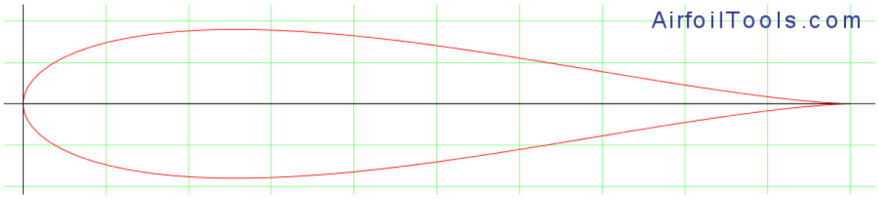

Figure 11: NACA 0183 Airfoil section profile

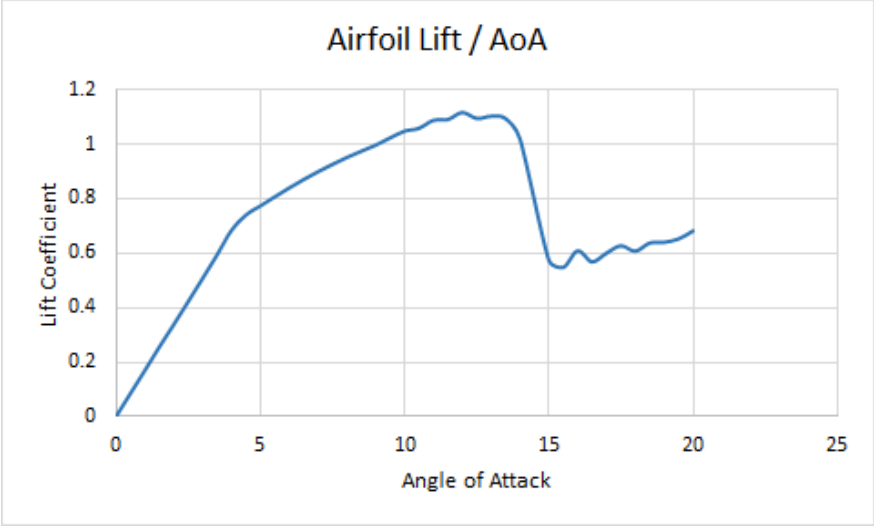

Figure 12: Lift Coefficient vs Angle of Attack. 5 kts at 20°C

Figures 12 show the Coefficient of Lift (CL) over a range of angle of attack for the wing cross section. Within the control software, the desirable angle of attack range for the wing is set between 8°and 12°. There

is however a risk of setting a 12°angle of attack because the wing stalls at about 14°. A transient fluctuation in wind direction could cause the sail to momentarily stall and slow forward progress. With a coefficient of lift of about 1, we were able to use our desired lifting force to solve for the surface area of the sail and subsequently the sail height. This resulted in a sail height of about 3m to produce a lifting force of 110 N. This lifting force was used to determine the horizontal moment on the boat at 25°of heel, as used in the above hull design calculations.

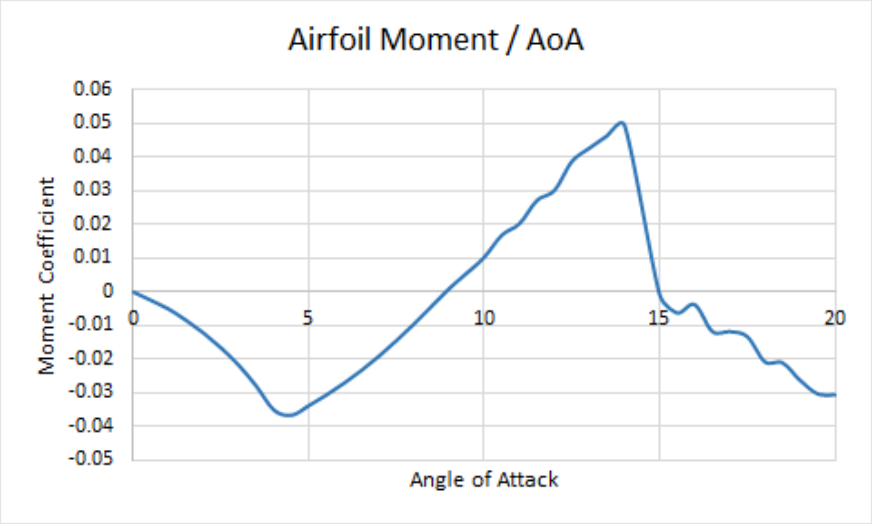

Figure 13: Moment Coefficient vs Angle of Attack. 5 kts at 20°C

Figure 13 shows the moments on the sail about its quarter chord point through the range of angles of attack (assuming positive moment to be the tendency to increase the angle of attack). From the graph, it is clear that the airfoil is balanced about the quarter chord point at approximately 8°. To account for this, we moved the located the mast near the quarter chord point of the wing, in order to theoretically balance the wing about the mast at an angle of attack of 8°. This is a rough estimate for a number of reasons. First, it neglects skin friction as well as forces applied by the trim tab and the trim tab arm. These calculations were simplified because a perfectly balanced sail is not a crucial feature. By shifting the the mast closer to the balance point of the wing, the power requirements for holding trim are reduced. However, some weathervane effect is desired to make the sail more controllable.

Trim Tab

The trim tab is a smaller servo actuated wing mounted aft of the main wing that controls the angle of attack using the moment generated by its mounting location and lifting force. With the same NACA 0183 section as the wing and a span of 1.16m it is capable of trimming the sail throughout its necessary angles of attack in as much wind as 15 kts and as little as 1.5 kts. The trim tab rotates about its quarter chord point, meaning that it is nearly balanced to decreasing the power draw from the servo.

Control System

To make the wing sail fully self contained, the control system was integrated into the joint between the upper and lower sections. This control box provides mounting for the trim tab arm, the wind direction sensor, actuation servo, and microcontroller. The wingsail connects to the rest of the boat over WiFi using an ESP8266 WiFi module to receive information about the desired point of sail. A Teensy 3.6 microcontroller then processes this information, and trims the sail to the optimal 8°angle of attack based on feedback from a wind vane. The wind vane is mounted on a low drag magnetic encoder, and located in front of the leading edge of the wing.

There are three possible sailing modes for the rigid wing: maximum lift, maximum drag, and minimum lift. The maximum lift mode is used when sailing upwind, and includes the option to reduce lift if the boat heels excessively. The maximum drag mode is used when sailing downwind, and results in the sail targeting an angle of attack of 90°. The minimum lift mode de-powers the sail, which is useful for the station keeping challenge, as well as providing a fail-safe operating mode.

4.1.3 – Cloth Sail

The cloth backup sail was designed around the same unstayed, free-standing, free-rotating mast as the wing sail. The sail is a full battened, square topped, high aspect ratio sail, constructed from composite mesh sailcloth. Thanks to sponsorship from Dimensional Polyant and Quantum Sails, the Sailbot team was able to design and produce a custom sail to fit the geometric constraints of the boat. The profile of the sail was designed to emulate modern performance sail profiles such as windsurfer and skiff sails. The new mainsail is designed to align its center of effort with the hull's center of lateral resistance, allowing the boat to sail balanced at 25°of heel. In addition to balancing the boat, the goal of this sail was to maximize the sail area to accommodate the low average wind speeds of Lake Quinsigamond.

Figure 14: Design Drawing and Final Version of the Cloth Sail

4.1.4 – Winch

The cloth sail requires a winch to control its angle of attack. The winches on previous WPI Sailbots exhibited a tendency to develop loose wraps around the winch drum or motor shaft when the sheet was slack. Loose wraps slid off the drum and lodged between the drum and housing, or wrapped over themselves, preventing further operation of the winch until the jams were manually cleared. To prevent these issues, the winch designed this year maintains constant contact between the sheet and powered drum. The design was based loosely on the concept of a self-tailing winch, where the sheet is controlled by some primary drum, and collected separately.

Conceptual Design

Sailbot teams at other schools addressed the loose wrap issue with a closed loop mounted on the deck, and driven by a shaft sealed through the deck (Figure 15). The sheet is then tied to a point on this loop, and guided through a fairlead. As the tie-off point moves farther from the fairlead, it pulls the clew of the sail

closer to the fairlead, trimming the sail. While this design is proven, it does occupy a significant amount of deck space.

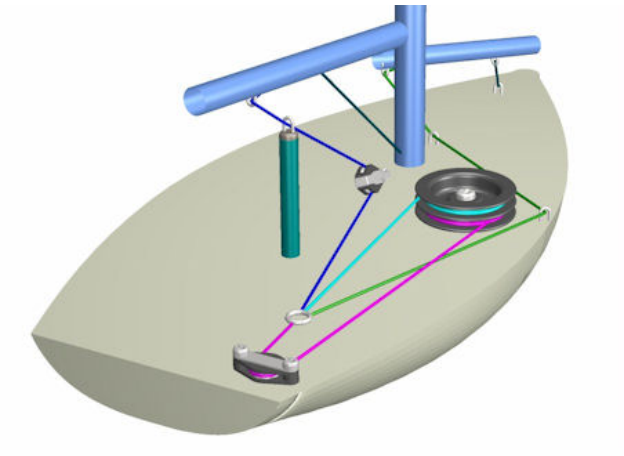

Figure 15: Winch Design Concept from [31]

Because we have two possible sail rigs, only one of which requires the winch, a self-contained winch that could be easily removed was a more attractive choice for our overall design.

Figure 16: Commercial Self-Tailing Winch [15]

Commercial self-tailing winches (Figure 16) are designed with toothed pulleys that bite into the large diameter yacht braid normally used as sheets on full size boat.

Figure 17: Prototype Winch Pulleys

Testing of a 3D printed version of this design indicated that the expected load on the mainsheet (Appendix B) would be insufficient to cause the teeth to "bite" into the sheet and prevent it from moving relative to the pulley. While the manufacturing method likely contributed to the ineffectiveness of this design, the design also did not completely fulfill the requirement of properly handling a slack mainsheet as it requires sheet tension to provide engagement with the teeth. To deal with a slack mainsheet, we designed a winch with a large, powered central drum surrounded by three compression rollers. The rollers press the sheet against the powered drum, maintaining constant contact between the sheet and the surface of the drum. The positive normal force provided by the rollers eliminates the need for tension in the sheet, allowing the winch to continue to operate with a slack sheet. In addition to preventing tangles, this winch design keeps all of the sheet above the deck, removing the possibility of water intrusion through the mainsheet fairlead.

Mechanical Design

We iterated the designs of the drum, rollers (Figure 18), and sheet to achieve the proper compression ratio without excessively loading the motor. An appropriate compression ratio is critical for the success of this design, as increasing the compression increases the frictional driving force between the sheet and the drum, but also increases the friction in the bushings supporting the drum and rollers. Experimentally, we found that a compression of 25% of the rope diameter was effective.

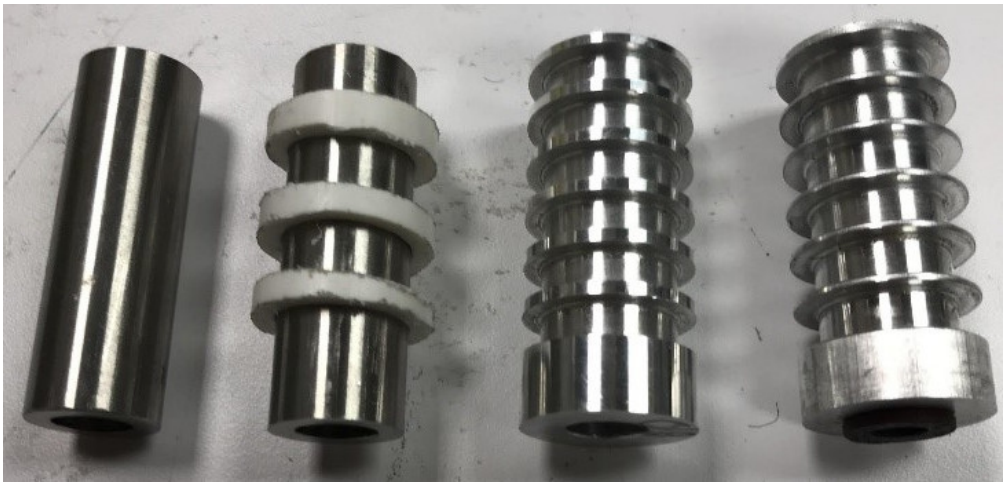

Figure 18: Winch Roller Iterations

The initial iteration of the design utilized a urethane conveyor roller from McMaster-Carr as the drive drum and smooth compression rollers. Testing showed that incoming sheet simply wrapped over the previous top wrap, rather than continuing to spiral down the drum. To maintain the spiral wrapping pattern and prevent overlap, we redesigned the rollers with a comb-like profile, with each tooth separating adjacent wraps. This spiral pattern stays in the same relative position around the drum, allowing for continuous operation. While this roller design did improve the separation of adjacent wraps, further testing showed that the thick rubber of the roller compressed, and allowed the wraps to "walk" between comb teeth, rather than sliding down the drum. To solve this issue, we machined an aluminum drum of the same size, and coated the driving surface in Plasti-Dip urethane coating to increase friction with the sheet compared to bare aluminum. The rigid drum surface maintains a constant compression ratio regardless of sheet loads, providing constant performance across the full operational range. We also added small, shallow grooves to the drum to help the comb teeth shift the wraps vertically.

After two turns around the drum, the sheet is guided off onto a spring driven drum that accumulates the loose sheet. The spring drum is powered by a constant-force spring, and is allowed to wrap randomly. As the sheet wrapping around the spring drum will be under constant tension, it will not develop loops that tangle themselves as previous winches have done. The height of the drum and limited number of wraps allows enough space for the addition of a future jib sheet if required.

The motor is mounted under the deck to keep it dry, and directly drives the drum. The shaft of the drum is sealed through the deck with a PTFE double-lip shaft seal. All of the winch components are mounted to a single aluminum plate. This self-contained design allows for easy removal when the wing sail is being used to save above-waterline weight. The sheet is routed through a set of pulleys mounted to the sensor mast on the stern of the boat to guide the sheet around the end of the movable ballast arm.

Motor Selection

The winch is actuated by a window lift motor from a Mazda RX-7. Peak mechanical power for this motor is approximately 13 watts, with a stall torque of 5.65 Nm at 12 amps and a free speed of 86 rpm. Emperical testing data can be found in Appendix C. Estimated mainsheet loads based on the sail used in 2017, of about 49N (see Appendix B) were used to size the winch drum at 63.5mm to place the motor near peak efficiency (about 38% of stall torque) under normal operation. This motor was chosen over similar motors because it has a compact form factor and includes an integrated encoder on the motor shaft. The integrated encoder simplifies position feedback, as there is no easily accessible mounting point for an external encoder. This motor and drum size combination did not require any additional reduction between the output of the motor and the drum, simplifying the mechanical design and resulting in a very compact unit. The drum size also gives us sufficient additional torque in case we encounter higher wind conditions that increase the sheet loads.

4.1.5 – Rudders

Based on previous experience, we identified the need for improved rudder authority when the boat is heeled. The wide beam of this boat makes a twin rudder system a reasonable approach, as the windward rudder can be mostly out of the water when the boat is sailing at the optimal 25°heel angle (Figure 19). The 2017 Sailbot compensated for the reduced authority when heeled by increasing the wetted area of the rudder, which also increases the skin drag of the rudder. For ease of transportation, the rudders were designed to be removed without any tools.

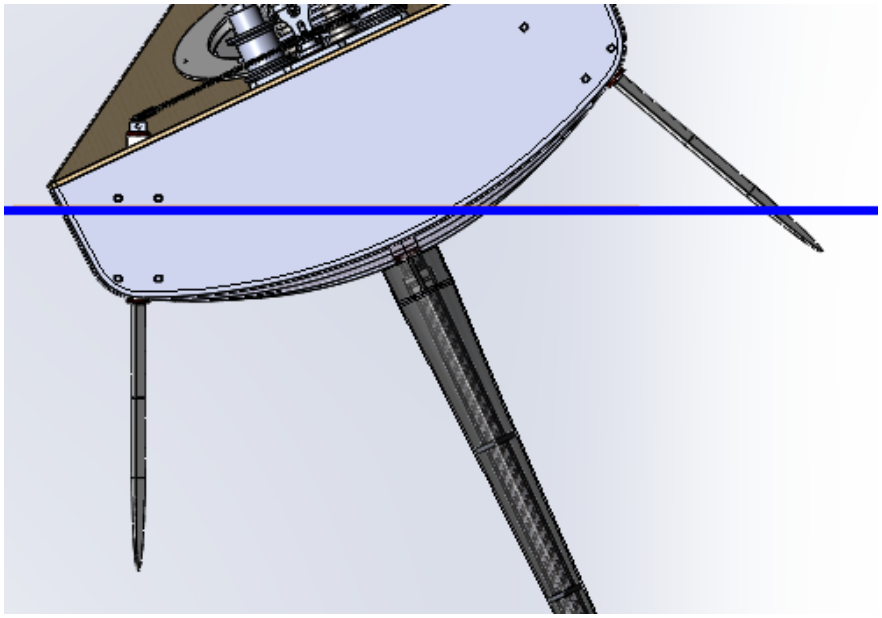

Figure 19: Rudder Submersion at 25°of Heel

Conceptual Design

Other twin rudder boats seen at previous Sailbot competitions steered the rudders independently, using a dedicated servo for each rudder. This design allows the windward rudder to remain stationary, reducing drag when the boat is heeled. Independently controlling the rudder angles also allows each rudder to be set to the optimal angle of attack when both are submerged, maximizing turning authority and minimizing drag. We decided however that using a single actuator to produce a single control output was a more elegant design. While the single actuator design removes the ability to set the windward rudder to zero angle of attack to minimize drag, the small submerged area and low angle of attack during normal sailing conditions meant that the drag from the windward rudder is small, and refining other areas of the design provided greater performance benefits.

Foil Shape and Size

The cross section selected for the rudder was a NACA 0012 section, a commonly used section due to its low drag and ability to the expected angles of attack without stalling. This section was chosen as it has been used successfully on previous similar boats. Use of a thicker section would allow higher angles of attack without stalling, and a more in-depth analysis of the choice of rudder section to improve performance is an avenue for further research in future iterations of this project. The pivot position was located at 25% of the chord of the rudder, just forward of the center of effort. This results in a mostly balanced rudder, with any unbalance tending to rotate the rudder toward the centered position. Balancing the rudder minimizes the torque required to actuate the rudder, reducing the overall power consumption of the system.

Online resources specified that the rudder area for full size boats should be about 6% of the submerged cross-sectional area of the hull, or 3-4% total for twin rudders. In comparison, last year's rudder, developed by USNA to use with that hull design, was approximately 29% of the submerged hull cross section. Using the full size boat specifications would result in a tiny, ineffective rudder. Accordingly, we chose to base our rudder size off of the scale of last year's boat, rather than full size boats. The area of one of the new rudders is 14.4% of the wetted cross section of the hull, approximately half of last year's. When both rudders are submerged (at low heel angles), the combined area is approximately equal to last year's rudder. This provides the same helm authority at low speeds, when the rudder surface area is most critical. Compared to the previous rudder, the effective area of each rudder will be decreased due to the offset mounting angle (an 11% decrease at zero degrees of heel), however the more balanced rig compensates for the decreased effective area.

Actuation Linkage Design and Analysis

The rudder actuation linkage was designed to provide nearly parallel motion across the full range of movement (shown in Figure 20). The final version of the linkage induces a slight positive Ackerman condition of 3.8°between the rudders at 45°of steering angle. The ideal Ackerman angle is 32°at the same 45°steering angle. Optimizing the Ackerman angle was not a design priority, as only one rudder should be submerged under normal steering conditions and an Ackerman steering system would only affect the rudder drag when both rudders are submerged. When both rudders are submerged, the boat is sailing at a small heel angle, and likely at low speed. These sailing conditions occur primarily during tacks, as the movable ballast system will ensure that the boat sails at a heel angle of 25°. As a result, the conditions where a full Ackerman steering system would significantly improve performance represent a very small proportion of the sailing time, and therefore little benefit toward overall performance.

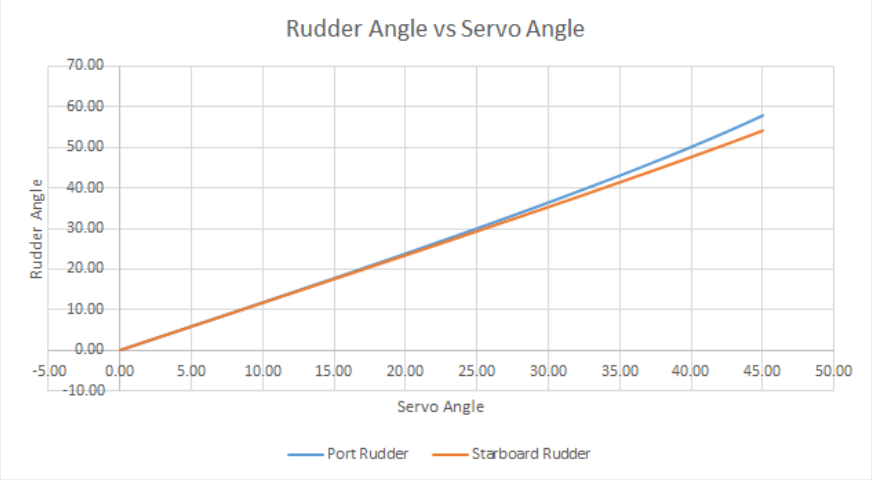

Figure 20: Absolute Rudder Angle vs Servo Angle

Because the rudder drive shafts and the servo output shaft are not parallel the linkage between the rudders and the servo must be compliant enough to prevent binding. We accomplished this using small ball joints, similar to those found in a car's steering mechanism (Figure 21). The range of motion of the ball joints provides the compliance required to prevent binding as the angle between the mounting screws varies across the full range of servo travel.

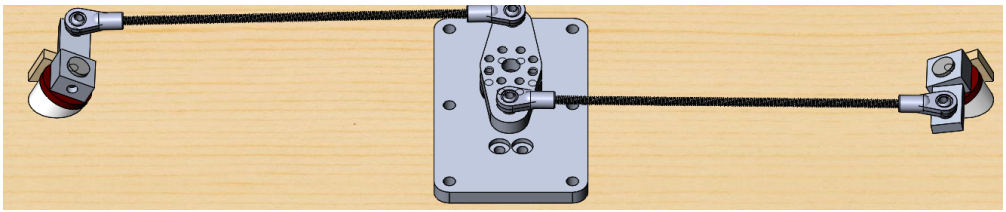

Figure 21: Rudder Linkage

To reduce the range of motion required from the ball joints, custom follower links were designed with a 25°angular offset between the rudder shaft and the mounting screw for the ball joint. This offset means that the ball joints are centered in their range of motion when the steering linkage is centered. These links couple to the rudder shafts with thumb screws, providing tool free installation, and the thumb screw provides clamping between the rudder shaft and the link, eliminating lash due to manufacturing tolerances. Figure 22 shows this follower link.

Figure 22: Rudder Follower Link

The rudder tubes were designed to be waterproof to prevent water ingress into the hull regardless of water level. The previous rudder systems used a rudder tube that ended above the waterline inside the hull of the boat. While this design was largely successful, it would fail the complete submersion waterproofing test, and a design that fully sealed the rudder tubes was required. The solution we developed was to seal the rudder tubes through both the hull and the deck, mounting the steering mechanism above deck level. The deck level mounting for the rudder horns also allows for easy attachment and detachment of the rudders without using tools, or having to access the inside of the boat. To keep the servo dry, the servo was mounted under the deck to a removable plate. An extended length servo horn passes through a bushing and PTFE rotary shaft seal in the plate to connect to the crank in the steering linkage. The couplers in the linkage were constructed from stainless steel threaded rod with nylon ball joints on the end. This construction was lightweight and inexpensive, with the only complex part being the rudder drive link with the offset angle.

4.1.6 – Keel

The keel is the lifting surface that extends into the water and holds a weighted ballast to stabilize the boat. Based on the results of last year's Sailbot, the keel needed increased surface area to improve authority at low speeds and separate configurations to balance the boat for each sail. We also chose to reduce depth and weight to ease rigging and transportation of the boat, and reduce boat weight.

Design and Specifications

The keel extends 1 m below the bottom of the hull, and has an area of approximately 0.215 m^2. Compared to the previous Sailbot, this design decreased the length by 40 cm and decreased the area by 0.027 m^2 (Figure 23). We used a flooded keel design to decrease the buoyancy of the keel while maintaining a large wetted area. The keel also uses the same NACA 0012 section as the rudders. This subsection provided the necessary thickness to accommodate the internal structure of the keel while maintaining low drag. Further research could explore alternative cross sections to improve performance. The shape of the keel bulb was based off of VO60 class designs from 2001, and the bottom was flattened to allow the keel to stand upright unsupported.

Figure 23: Previous Keel Compared to New Keel

The hull design incorporates two locations for the keel to attach, one for each type of sail. The lift calculations for the rigid wing sail in average Lake Quinsigamond conditions calls for the center of lift of the keel to be located 38 cm behind the mast. Similarly, the calculated location for the design of the cloth sail is 53 cm behind the mast for the same sailing conditions. The keel is raked at a 20˚angle to reduce the distance between the mast and keel boxes. The keel box and mast step area is the most highly stressed area of the boat, so reducing the size of this area improves the strength and stiffness without requiring a large, heavy internal structure. A cutaway view of this area is shown in Figure 24. The keel core passes through three layers of plywood that are attached securely to the hull with structural filler, as well as being attached to the adjacent rib subsections with interlocking tabs.

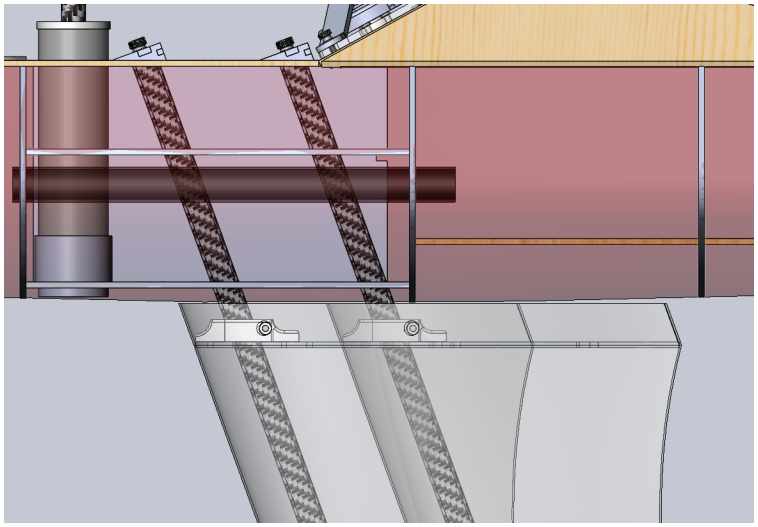

Figure 24: Keel Tube Locations

Analysis

To calculate the weight of the ballast, we used a simplified equation from previous robotic sailing research [5]. This calculation does not include hull stability because the shape of the hull was not finalized at the time. However, the additional stability provides more righting moment, and therefore provides a safety factor for unexpected conditions. The equation for this calculation is:

$$\sum M_c = w_k \sin(\theta) l_k - d_s(f_s + w_s \sin(\theta)) - d_k f_k = 0 \tag{4.1}$$

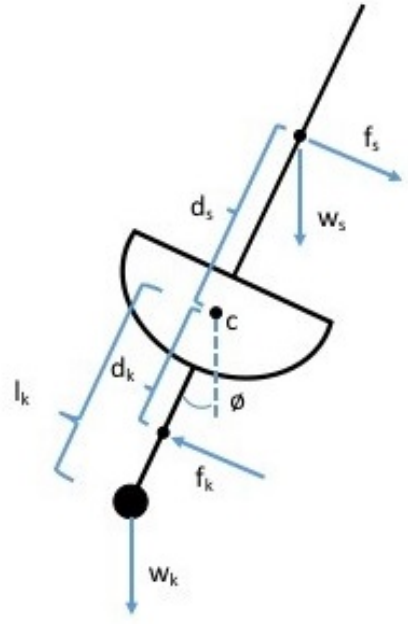

Figure 25: Free Body Diagram of a Heeling Sailboat

Table 1: Variable descriptions for the free body diagram of a heeling sailboat

Variable	Description
c	Center of rotation of the boat
θ	Heel angle of the boat
d_s	Distance to the center of effort of the sail
f_s	Force of the sail
w_s	Weight of the sail
d_k	Distance to the center of effort of the sail
f_k	Force of the keel
w_k	Weight of the keel
l_k	Distance to the center of gravity of the keel

For these calculations, we used the weight of the previous wing sail as w_s, 45 degrees as ø, and the maximum force of the cloth sail with 8.5 kts of wind (the maximum wind speed expected in testing conditions) as f_s. We assumed that d_s is approximately half the height of the sail, that d_k is approximately half the length of the keel, and that $f * s = f_k$. This resulted in a desired moment of the keel of 121.9 Nm. Using an l_k of 1.11m we calculated a keel weight of 109.8 N. Accounting for the buoyant force on the keel, the final desired keel weight was 132.2 N. However, additional material needed to stiffen the keel resulted in an overall weight of 158 N, compared to the previous weight of 170 N. This weight reduction meets our project goals, but additional research could explore a lighter keel design that maintains adequate stiffness.

The original design for the keel (square carbon fiber core, with machined PETG ribs and a thin polycarbonate skin) proved to be too flexible, and bent significantly under the weight of the bulb. To reduce the flexibility of the keel, we wrapped the carbon fiber core with 4 additional layers of fiberglass and then attached an additional length of a round carbon fiber tube wrapped on to it, separated by 3D printed spacers. This additional stiffness concentrated the stress at the joint between the keel and the hull, so we added an 20 cm aluminum insert inside the carbon fiber tube. A Finite Element Analysis estimates that the deflection is reduced almost 10x at 25°of heel. In addition, we rebuilt the keel skin with fiberglass and adhesive filler wrapped over laser cut acrylic ribs, providing additional stiffness to the keel. We also reinforced the carbon fiber tube at the stress concentration where the keel enters the hull with an internal aluminum section epoxied into place. This aluminum section prevents the carbon fiber from being crushed, as well as increasing the cross sectional area at the stress concentration.

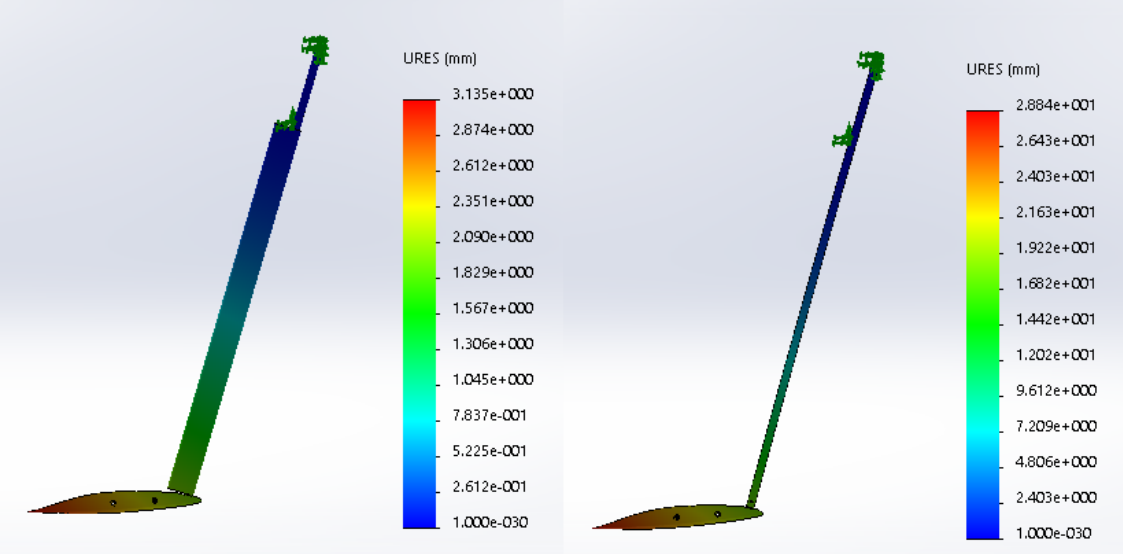

Figure 26: Stiffened Keel Core FEA Comparison

4.1.7 – Movable Ballast

Controlling the heel angle of the boat is critical, as the boat is designed to sail optimally at 25°of heel. Less heel increases the drag of the hull, and more heel decreases the effectiveness of the sail. The movable ballast system is designed to be capable of keeping the boat at 25°of heel at seven knots of wind (the average wind speed in Worcester). It is also able to correct the boat's heel within five degrees of the desired position in five seconds.

Conceptual Design

The movable ballast system was designed to keep the ballast weight as close to the water line as possible, while still maintaining the proper moment. The deck and arm are both angled at 25°, so as the boat heels, the arm of the ballast will remain relatively parallel to the water (Figure 27). The arm bends in the middle to accommodate the raised deck that provides the angular offset and houses the gearbox.

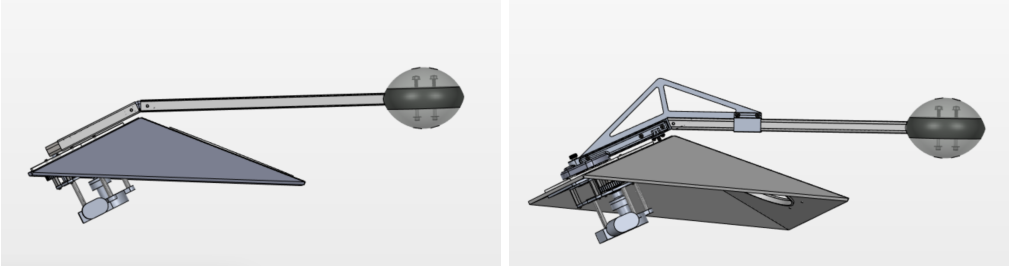

Figure 27: Movable Ballast Iterations 1 and 2

Heeling Moment Analysis

The moment needed for the movable ballast was calculated by extending the calculations for the keel to include an additional moment arm parallel to the waterline. Using the previously calculated weight of the keel, and a ø of 25°instead of 45°, we determined the additional moment necessary to keep the boat at the desired angle in the same wind conditions using the following formula, where l_a is the length of the moment arm and w_a is the weight of the movable ballast.

$$\sum M_c = w_k \sin(\theta) l_k - d_s(f_s + w_s \sin(\theta)) - d_k f_k + l_a w_a = 0 \tag{4.2}$$

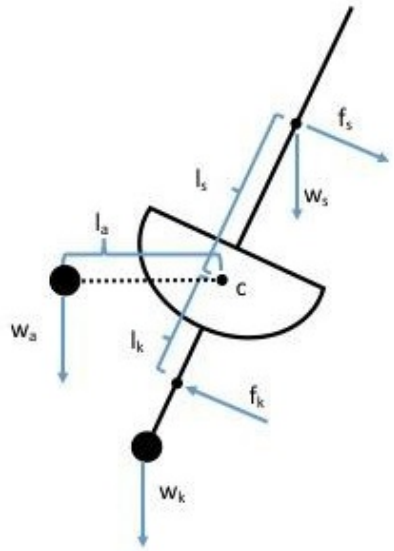

Figure 28: Free Body Diagram of a Boat with a Movable Ballast System

At a heel angle of 25°and with a maximum arm length of 65.8 cm, the weight of the ballast is equal to 90 N. This maximum length was determined by the available space between the sensor tower and the keel box. Additionally, the weight of the ballast is configurable, with three different sections to accommodate a range of wind speeds.

The movable ballast reduces the overall weight of the system by increasing the effective moment arm of some of the ballast, therefore decreasing the total weight needed to provide the correct righting moment. When factoring in the weight of the actuator and gearbox, the movable ballast system reduces the mass of our boat by an estimated 13 N, about 6% of the fully rigged weight of the boat.

Motor Selection

Based on the arm length and weight selected, we identified that we needed a motor with approximately 22 watts of power to provide the performance we required. The motor we selected is a window lift motor with an integrated non-backdrivable worm gearbox. The non-backdrivable worm drive allows the movable ballast arm to maintain a set position without the need to power the motor. This improves the stability of the control system, as the control loop does not have to constantly maintain the arm position which would require high gains to compensate for small deflections. The position holding ability also saves power, as the motor can be shut off once the heel angle of the boat reaches steady-state at the desired heel angle.

Gear Train Analysis

Initial calculations indicated that an additional reduction of approximately 8:1 between the motor output and the movable ballast arm was required. Under the peak loading condition (which occurs at 90 degrees of heel with the movable ballast arm along the centerline of the boat, shown in Figure 29), this gear ratio results in a motor torque approximately half of stall torque, which is the peak power state. While this condition should never occur while sailing, it does provide a useful upper bound for evaluating performance.

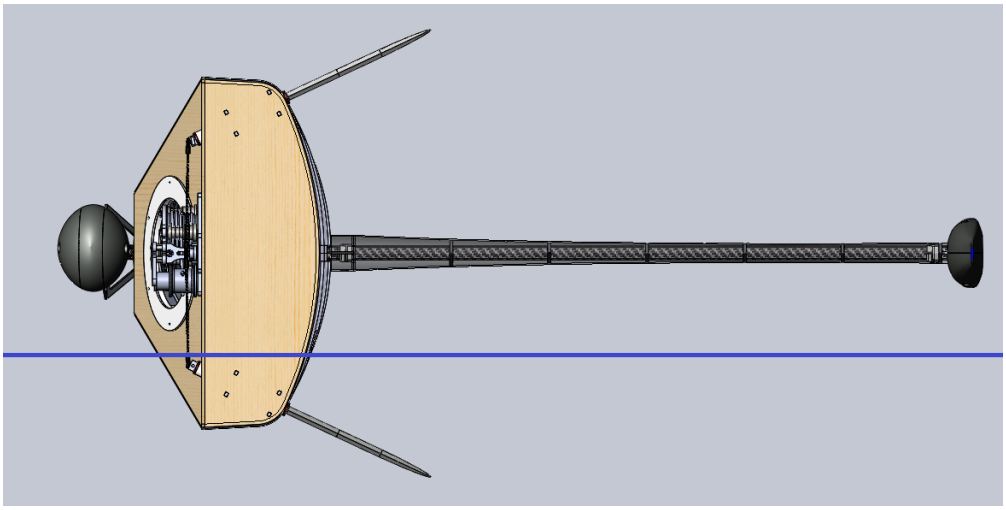

Figure 29: Maximum Possible Movable Ballast Loading Condition

To obtain this reduction we designed a custom two stage spur gear system (Figure 30) with an overall reduction of 8.35:1 using gears from VEX Robotics. These gears are manufactured from 7075 aluminum, a strong, lightweight, and corrosion resistant aluminum alloy.

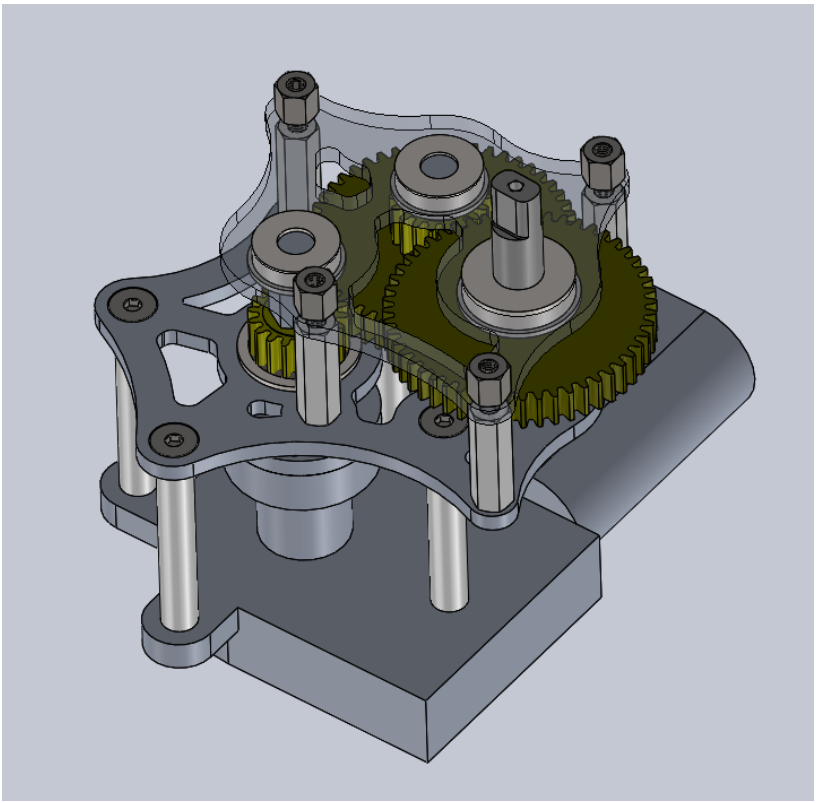

Figure 30: Original Movable Ballast Gearbox

Upon testing, we identified large variations in speed based on load, and that smoother operation was desirable. The analysis for the initial design was a purely static analysis, for steady-state operation. It

did not consider starting torque, dynamic loads, or the current draw. To improve performance and reduce current draw, the gearbox was redesigned with a higher torque ratio, which moves the motor to the left on the speed/torque curve. This lowers the torque required from the motor (seen in Figure 31), and increases the speed of the arm under peak load. Under low load, the arm operates at a lower speed, making the speed of the arm under all conditions more linear, as seen in Figure 32.

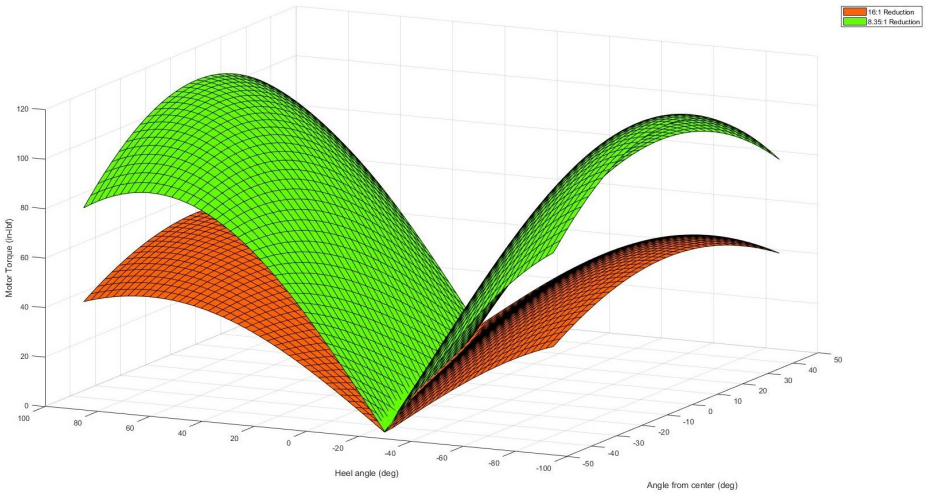

Figure 31: Motor Torque Comparison

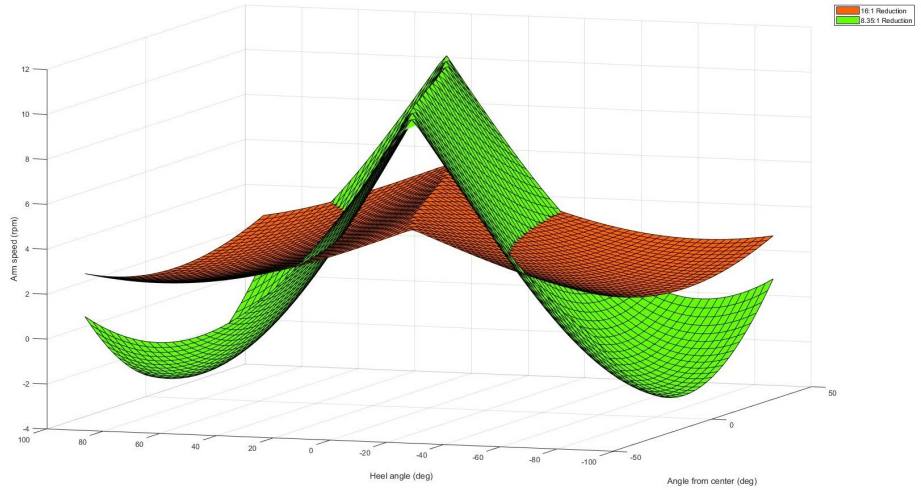

Figure 32: Arm Speed Comparison

The green plot shows the motor torque requirement over the full range of heel angles and movable ballast operating angles with the initial gearing. The orange plot shows the torque requirement for a 16:1 reduction, the revised gear ratio. This specific gear ratio was selected because it has a peak current draw of 20.5A under the peak loading condition for the maximum weight of the movable ballast arm. This maximum current is under the maximum continuous current draw limit for the motor controllers, putting nominal operation (even under maximum load) well within the capabilities of the motor controllers. The gears selected to achieve this reduction were 16 and 64 tooth VEXPro gears. The gear spacing for these gears also allows one or both stages to be swapped for 14:66 gears instead of 16:64, increasing the ratio to 18.85:1 or 22.22:1 if additional

reduction is required. The 14 and 16 tooth gears from VEX are available in 4140 steel, which has a 25% higher shear strength (413 MPa for 4140 steel[40] [1] vs 331 MPa for 7075 Aluminum [2]). This is important for the small pinion gears, as the 14.5 degree pressure angle of the VEX gears results in undercutting and small root thicknesses for small gears.

Movable Ballast Arm Design and Analysis

The section of the arm that couples to the motor is a machined aluminum I-beam, with a triangular truss that connects to both the I-beam and carbon fiber rod (Figure 33). The aluminum link also provided the ability to add an integrated roller near the joint to transfer some of the load to the deck, significantly reducing the bending moment on the shaft. In an effort to minimize the weight of the movable ballast system, the initial arm was designed as two square carbon fiber links, coupled with a welded stainless steel joint. However, the coupler fit loosely in the tubing, and the length to diameter ratio was too small to provide enough stiffness, leading to the arm hitting the deck.

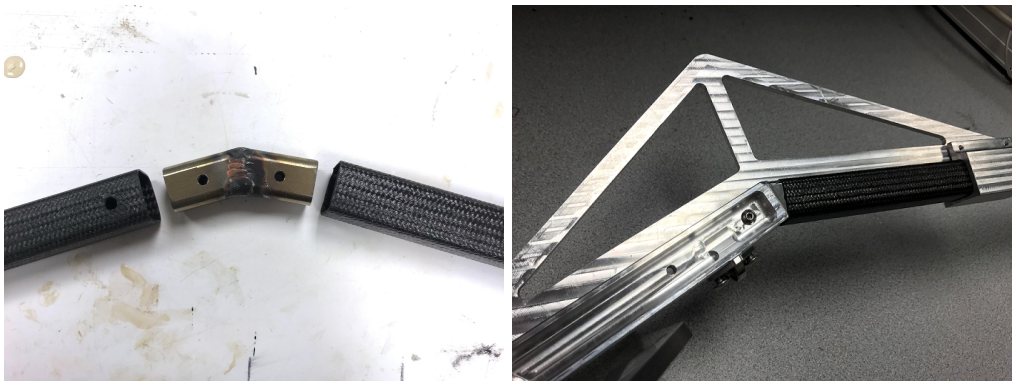

Figure 33: Original Coupler Design vs Revised

In order to verify the strength and deflection of this coupler under load, Finite Element Analysis was performed on individual parts, and the assembly as a whole. The stiffness of the arm was the key design consideration, to prevent excessive deflection under both static and dynamic loads. Excessive deflection could cause the arm to collide with the aft sensor mount, or induce undesirable dynamic effects to the pitch or heel motion of the boat. To simplify the analysis, the portion of the gearbox under the deck was treated as a rigid body after being analyzed separately.

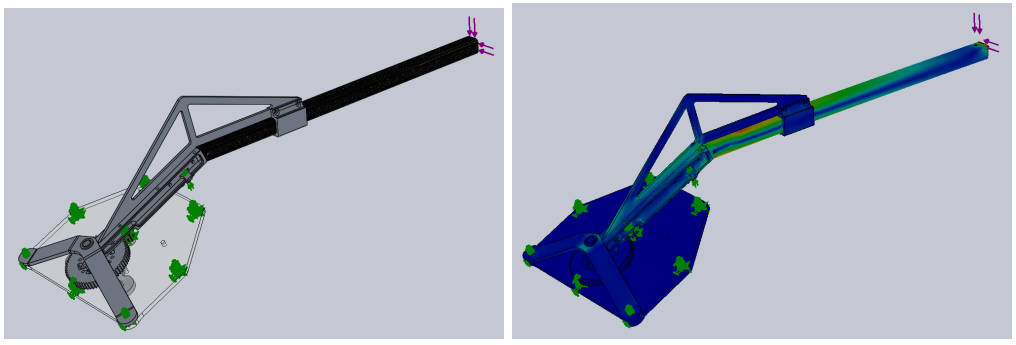

Figure 34: FEA of Movable Ballast Assembly

Under double the maximum static load (133N of static load, plus 133N to account for dynamic effects) the tip of the arm deflects just 15mm. The movable ballast arm was also simulated with a horizontal side

load, to analyze performance when the boat is heeled. Under a combined load of 267N vertical and 334N from the side, the arm deflects 57mm. This loading condition emulates the loads that the movable ballast would experience when the boat is heeled and the arm is partially rotated, and includes some allowance for dynamic effects from waves that could cause the movable ballast to bounce. Although this deflection is more than twice the vertical deflection, it only exists in a transient state. The arm should be approximately horizontal at steady state, so horizontal stiffness was not a critical design consideration.

The other critical point identified for analysis was the strength of the gear teeth at the final reduction. The teeth of the pinion the drive the final output gear are under significant stress due to their small size and high load (Figure 35). Analysis revealed that under the combined vertical load of 267N and side load of 334N, the gear teeth had a safety factor of 1.25, confirming that they had sufficient strength to handle the applied load.

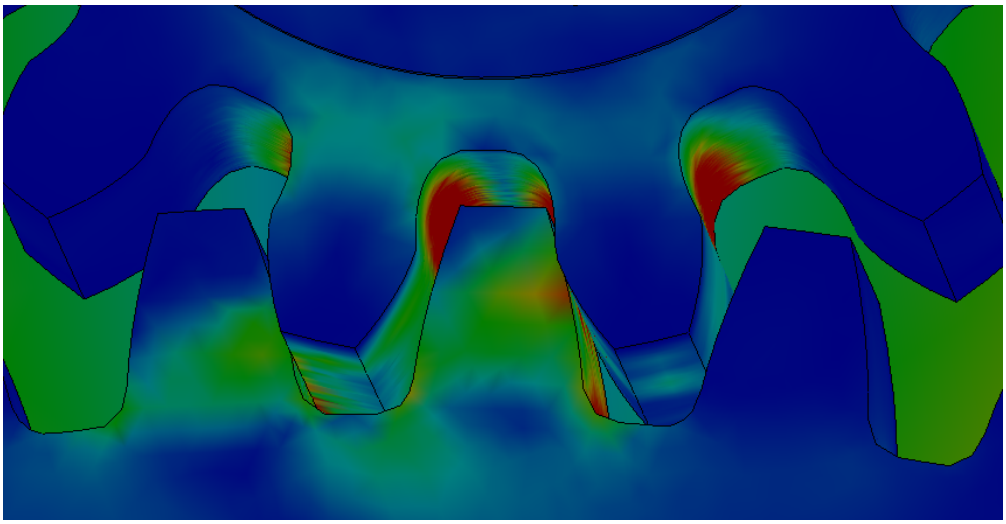

Figure 35: Gear Tooth FEA

A key design consideration for the movable ballast arm was the connection between the gearbox and the movable ballast arm. The initial design for the full carbon fiber arm simply mated a double D shaft from the output of the gearbox to a matching slot on the arm, with an axial thumbscrew for retention (Figure 36).

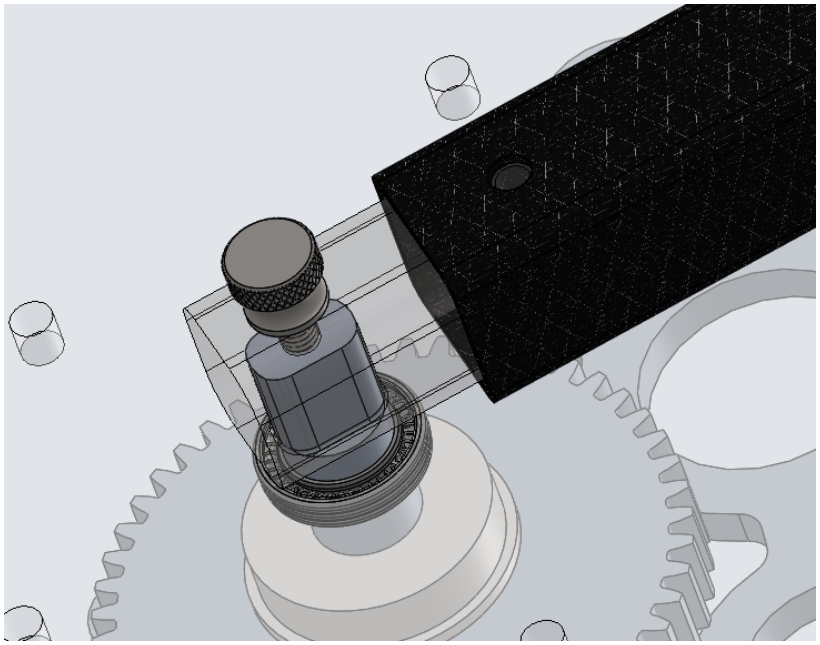

Figure 36: Original Double-D shaft coupling

While this was simple to manufacture, the sharp transition between the round shaft and double D created a stress concentration in the aluminum shaft, and we had concerns about the aluminum shaft and pocket wearing due to the highly dynamic loading the joint experiences. As the connection wore, the increased clearance between the shaft and pocket would increase any lash, and allow for relative motion that would increase the dynamic loading. Multiple other shaft couplings were designed, involving tapers and clamps that would allow the coupling to account for any wear that developed, seen in Figure 37.

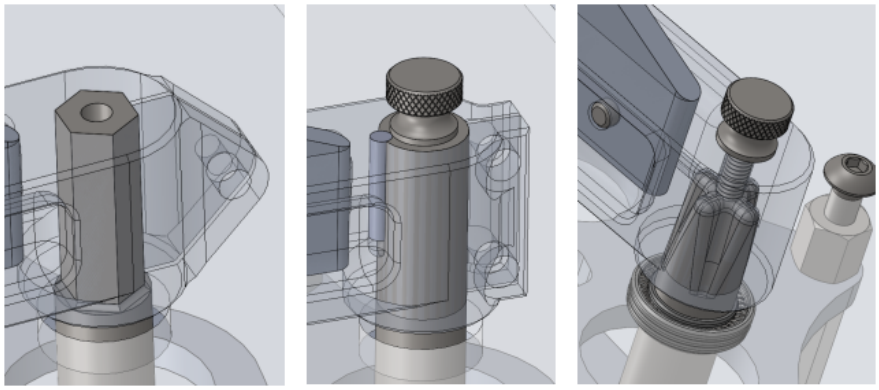

Figure 37: Original Double-D shaft coupling

However, these were complex to machine, and provided small load bearing surfaces that were still likely to wear over time. To solve this problem, the final stage of reduction was moved above the deck, and the final driven gear fixed to the aluminum arm. The first stage of reduction remained under the deck, and the intermediate idler shaft passes through a rotary shaft seal in the deck to keep the interface waterproof.

To securely mount the shaft pivot, an acetal bushing with a blind hole was machined and mounted in the deck plate. The blind bushing maintains a watertight interface for the shaft, and was sealed to the mounting plate with a flexible, waterproof adhesive. A cross section of this arrangement is shown in Figure 38.

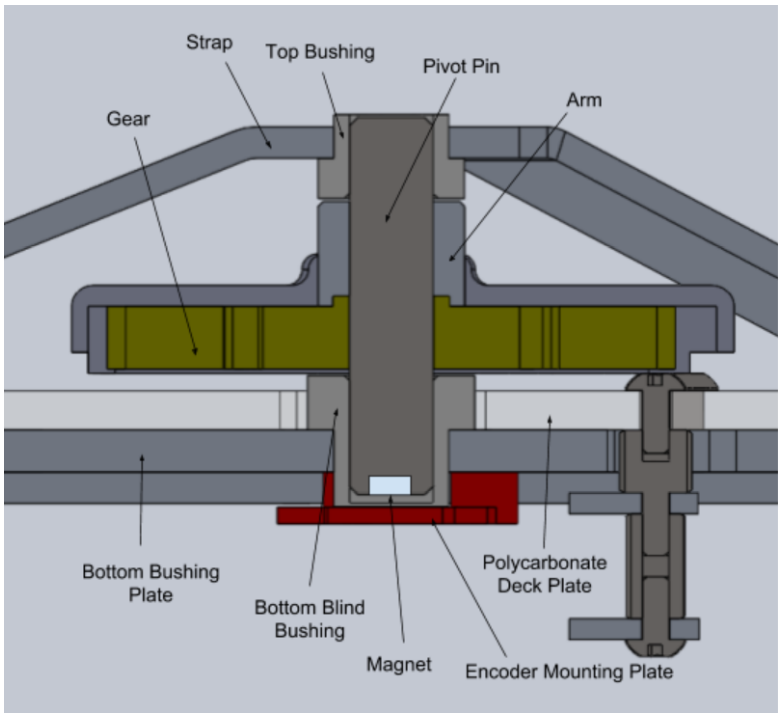

Figure 38: Arm Mounting Cross Subsection

The primary load on the bottom bushing is radial, as the axial load is upward, away from the deck. To axially retain the movable ballast arm, a strap was designed with an additional acetal bushing, and affixed to the deck with thumbscrews. The thumbscrews allow for easy removal of the arm for transportation of the boat.

The position of the movable ballast arm is sensed with an AMS5048 absolute magnetic encoder on a custom breakout board. The magnet for the encoder is glued into the end of the pin that the arm pivots on, providing absolute position feedback for the arm. In addition, we use a MXC6244AU thermal inclinometer to detect the heel of the boat as feedback for the movable ballast control algorithm.

Ballast Control

The movable ballast control consists of two nested PID loops. The outer loop determines the desired heel angle based on the wind direction and calculates a goal arm angle to produce that heel. The inner loop uses the arm angle to send desired voltages to the ballast motor controller over the CAN bus. The motor controller executes these voltages, as well as transmits the arm angle and heel angle feedback over the CAN bus.

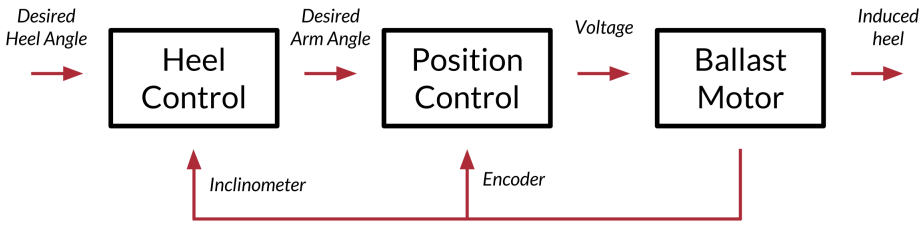

Figure 39: Ballast Control Loops

One method we explored for improving arm response was additional feed-forward control based on the heel and arm angles. Since the heel of the boat and angle of the arm directly affect the torque required to move the arm, it is important to factor these biases into the control algorithm. We experimentally determined values for these feed forward terms by testing the voltage required to overcome static friction at several different heel and arm angles. We tested the voltage required to move the ballast in each direction at heel angles of -25, -15, 0, 15, and 25 degrees and arm angles of -45, 0, and 45 degrees. We tested each combination five times, and then found a linear fit for both heel and arm angles. The resulting gains were 0.0457 volts per degree of heel and 0.0334 volts per degree of arm angle. Figure 40 shows the ballast response before and after gravity compensation. The chart on the right shows that gravity compensation improves the settling time of the ballast control.

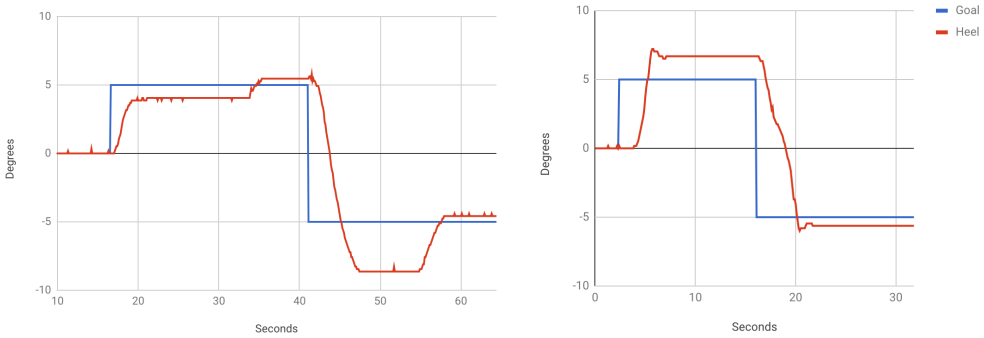

Figure 40: Ballast Control Performance Before and After Gravity Compensation

Furthermore, gravity compensation testing revealed a deadband between -2.24 and 3.09 V at 0 degrees of heel and arm angle, where applied voltage cannot overcome static friction in the arm. Using the above feed-forward terms, we can reduce overall power consumption by reducing outputs in part or all of this range to 0 V.

4.2 – Electrical System

4.2.1 – Ballast and Winch Motor Controllers

In order to control large electrical motors on the boat, we required motor controllers that communicate with the main processor. These motor controllers must be capable of communicating over CAN on the shared NMEA2000 bus, and capable of supplying the power required to drive the motors under their max loading conditions.These motor controllers must also be waterproof, and provide an interface for connecting external position sensors.

Power Supply

The NMEA2000 standard does not specify maximums for current draw or bus supply voltage noise. However, a common retailer for NMEA2000 connectors [25], specifies the maximum rated current for the highest power network connectors at 9 amps. A 9 amp maximum current draw places a significant limitation on the rate at which the control devices can respond as it limits the total power draw of the boat at any time to a maximum of 108 watts (12V * 9 amps). To bypass this issue, we utilized a separate power bus for high current applications.

Existing Options

While there are commercially available CAN motor controllers, none meet all of our design criteria for use on the sailboat. The Talon SRX is a reliable CAN bus motor controller that is commonly used by FIRST Robotics competition teams. It is rated for 60A continuous current draw, a burst current draw of 100A, 60V

maximum input, is conformally coated and sealed, and has built-in safety functions, current monitoring, and external sensor input [43]. However, the CAN communications protocol is not readily available and must be reverse engineered from online sources such as [30]. Furthermore, the external sensor input does not support a sensor with an I^2C or SPI based protocol [43]. Another series of motor controllers used in other WPI robotics projects is the Maxon Motor DC Motor controllers. Maxon Motor has several motor controllers that can communicate over a shared CAN bus, and handle the power required for systems on the boat [32]. However, these controllers are prohibitively expensive, and are completely exposed without any protection from water intrusion. Roboteq also offers a line of motor controllers that are able to communicate on a shared CAN bus and some motor controllers are rated for the power draw of our applications. However, none of their products offer any protection from water intrusion, nor do they have any interface options for I^2C or SPI based external sensors [6]. Because none of the commercially available options for motor controllers matched our criteria, we chose to design our own.

Previous Work

Last year's team reached the same conclusion concerning commercially available motor controllers, designing a custom unit using an ATmega328p microcontroller running off of an internal 8 MHz clock, a VNH2SP30 motor driver IC, and an MCP2515 CAN controller for interfacing between the microcontroller and the CAN bus using SPI [49] With the Optiboot bootloader, the microcontroller could be programmed with the popular Arduino IDE. This made developing and deploying code relatively simple. The MCP2515 appeared to perform reliably, and made interfacing with the CAN bus relatively simple. However, the VNH2SP30 motor driver was never used on the final version of the boat due to inconsistent performance during testing. The VNH2SP30 offered fault monitoring and current sense output pins, however these features were not fully implemented despite the benefits for safety monitoring and debugging. In the competition version of the 2017 Sailbot, a PWM based motor controller was used to drive the winch motor, and the custom motor controller provided a means of controlling the rudder servo with PWM over the CAN bus.

Microcontroller Selection

Because the motor controller was being redesigned, we evaluated several options for microcontrollers that offered more features that the ATMEGA328p. After looking at several different vendors and comparing various options, we chose the STMicroelectronics STM32f042k6 microcontroller primarily for its built-in CAN peripheral. The CAN peripheral allows the device to interface with a CAN bus without any external hardware beyond the standard CAN transceiver to supply the correct line voltages and isolation [41]. The cost of this microcontroller was also less than the combined cost of the ATMEGA328p and MCP2515 CAN interface ($2.83 vs $1.32 + $1.91). While both MCUs have an internal 8 MHz oscillator, the STM32f042k6 can multiply the clock frequency to higher speeds than the ATMEGA328p, and can use an external oscillator that runs at up to 32 MHz. The ATMEGA328p is limited to 20 MHz under ideal conditions, and is limited to 16 MHz in standard implementations. Having a microcontroller with higher possible clock speeds will allow for the possibility of more complex control systems to be deployed to the microcontroller and allow the control law to operate on a more deterministic processor when compared to the control law implemented in the BeagleBone in the 2017 Sailbot. Although there were several other lower cost microcontrollers that fit the criteria for the new revision, the STM32f042k6 was selected for its cost in low quantities, the availability of software from the manufacturer to configure the chip without specialty programmers, the availability of free code compilers that can run on Linux based systems from several sources [38] [14], and the availability of a development board for prototyping the new revision.

Motor Driver Selection

Using a driver IC rather than implementing an H-bridge circuit from discrete components provides all of the desired features, while reducing PCB footprint, design complexity, and debug time. As mentioned previously, the VNH2SP30 DC motor driver IC was used in the original implementation of the custom motor controller. This driver IC could not be directly used with the STM microcontroller due to a difference in logic signalling levels (3.3V for the STM32f042k6 and 5V for the VNH2SP30). Although logic level converters could have been used, this would have increased the footprint required for the PCB and increased the complexity of the

system. To meet the power requirements of the movable ballast and winch, a motor driver that could operate from the 12V battery power on the boat, and could handle at least 28 Amp bursts of current (stall current of the movable ballast). After researching several options for a new DC motor driver IC, the VNH5019A-E H-bridge motor driver IC from STMicroelectronics was selected for its built-in current sensing, thermal limit protection, low gate resistance, and 3.3v logic levels. Of the available motor driver ICs, only the VNH line from STM offered integrated current sensing. Current sensing and thermal limit protection prevent the motor controller from self destructing, while low gate resistance maximizes efficiency and reduces the heat sinking requirement.

Thermal Analysis

In order to validate that the selected motor driver IC would be able to remain operational during normal conditions, a thermal analysis was conducted to ensure that the device would not exceed the internal thermal limits of the part. The datasheet for the VNH5019A-E lists the thermal resistance to the surrounding air in terms of the amount of copper area connected to the power supply input and both motor output channels. To determine worst case scenarios, the minimum recommended copper area of 4 cm2 was used in the calculations. With this amount of copper area for dissipating thermal energy, the thermal resistance of the chip for the high-side driver is approximately 33°C/W and the thermal resistance of the combined high-side and low-side drivers is approximately 11°C/W. The datasheet lists the formula for calculating the temperature of the chip as

$$T = P * R_{ths} + P * R_{thsls} + T_{amb} \tag{4.3}$$

where P is the power conducted through the driver IC, R_{ths} is the high-side thermal resistance, R_{thsls} is the combined thermal resistance of the high-side and low-side drivers, and T_{amb} is the ambient temperature of the surroundings. The datasheet also lists a range of temperatures that the driver IC will internally shutdown the high-side and low-side drivers at with a minimum temperature of 150°C, a typical temperature of 175°C, and a maximum temperature of 200°C. This temperature cutoff varies between different VNH5019A-E devices, so the worst case condition of a 150°C shutoff is considered. The provided calculations will determine the maximum continuous power throughput, and in order to determine the maximum continuous current throughput, the resistance of each leg was used. The datasheet lists the fully saturated resistance of each leg of the H-bridge as 18 mOhms. Historical weather data for Worcester, Massachusetts in early June was also used to determine some approximate worst-case conditions for the ambient temperature. In early June, the worst case temperatures for the past 5 years is approximately 36°C, with typical temperatures around 26°C [48]. Although the motor controllers will be operating in a metallic case inside of the boat, it is assumed that the internal temperature of the hull will closely match the ambient temperature of the environment. This simplifies thermal calculations to determine some approximations of maximum sustained current that the motor controllers can achieve during these conditions. In the worst case conditions of 36°C ambient temperature, and thermal cutoff of 150°C, the motor driver is able to sustain:

$$(150C - 36C)/(33C/W + 11C/W) = 2.59W \tag{4.4}$$

Using the high-side and low-side saturated resistances the maximum continuous current is:

$$\sqrt{2.59W/(18mOhm + 18mOhm)} = 8.48Amps \tag{4.5}$$

In the expected temperature conditions of 26°C ambient temperature, and thermal cutoff of 175°C, the motor driver is able to sustain:

$$(175C - 36C)/(33C/W + 11C/W) = 3.39W \tag{4.6}$$

The maximum continuous current in these conditions is:

$$\sqrt{3.39W/(18mOhm + 18mOhm)} = 9.70Amps \tag{4.7}$$

Even in the worst case conditions, the selected motor driver should be able to continuously operate the the winch and movable ballast. Although the maximum continuous current for this motor driver is below the maximum currents of both systems, both systems are operated intermittently, with duty cycles that are likely well under 50%. This allows some time for the driver to cool and remain within the thermally limited conditions.

Voltage Regulator and CAN Transceiver

The design criteria for selecting both the voltage regulator and CAN transceiver were relatively simplistic. The voltage regulator was selected from designs that have been used successfully from Sparkfun. Although we could have optimized the selection across criteria such as cost, and power output, there was little benefit in doing so. To ensure that the selected voltage regulator would have enough current output, we combined the maximum current draw of the microcontroller, status indicator LEDs, CAN transceiver, temperature sensing circuit, and motor driver logic, and ensured that the total did not exceed the maximum current output for the device. The CAN transceiver was selected with similar reasoning, using a transceiver that was used previously on a development board for prototyping and on the BeagleBone in the 2017 Sailbot.

PCB Design

Because the selected microcontroller has an integrated CAN peripheral, several optimizations could be made to the original layout, and the goal for the PCB design was to reduce the board size from the original design. See Appendix D for the final schematic and PCB design for the new custom motor controller.

4.2.2 – Rudder Servo

For the 2017 Sailbot, the custom motor controller also acted as a interface between the CAN bus and the PWM signals required for the rudder servo. Although this implementation worked in practice, we wanted to be able to receive feedback on the internal state of the rudder servo, as well as be able to tune the control gains and implement custom control laws. This would allow us to better refine the control of the rudder as well as see live telemetry to do in-field debugging of the rudder servo. To accomplish this, we chose to refit a commercial servo with a custom control board, reusing all of the existing mechanical components. Although the winch and movable ballast have significantly higher power requirements than the servo, the main architecture for the controller is the same. Since these architectures are very similar, we decided to mostly replicate the design of the custom motor controller in the custom servo controller with some optimizations for space. By keeping the same microcontroller and only changing the IC package size, we are able to maintain similar code between all three custom motor control devices on the boat.

Driver Selection

The driver IC selected for the motor controller was too large to fit inside of the case of the servo, and was able to handle significantly more power than was necessary for the rudder servo. To determine the driver requirements for the motor already installed in the servo, we stalled the motor to determine the current ratings that the driver IC needed. When stalled at 12V, the servo drew 3.06 Amps, and drew 0.14 Amps under no load. Ideally the servo operates well below the stall current, so we chose to select drivers that have a maximum current rating of at least 1.5 Amps. The desire to have built-in current sensing to reduce the PCB footprint was even further emphasized due to the small area inside of the servo case that we had to work with. TI was the only manufacturer that had driver ICs with built-in current sensing in the approximate power output range that we needed, and we chose the DRV8801 for its cost and availability of single quantities at the time. There were other options available, but they were either more expensive, or not available in single quantities within our time frame.

Board Design

The PCB design and layout for this servo controller replacement was heavily driven by dimensional constraints to fit inside of the servo case. The board was designed so that it could be dropped into a custom servo housing that provides mounting for the NMEA connector. We originally considered using the same AMS5048 absolute magnetic encoder used with the movable ballast in the servo. The mechanical limits of the servo could then be removed, and the servo could rotate a full 360^{o} without limitations. However, adding all of these components on a single PCB was not possible, since the sensor needed to be mounted separately from the motor driver IC to reduce interference. Adding the magnet to the output shaft also presented a significant manufacturing challenge due to the very small size and very tight tolerances. Instead, the existing potentiometer was used, and a 3 conductor cable was soldered between the potentiometer and 3 pads on

the top of the PCB board. See Appendix E for the final revision of the new servo control board, and the dimensional constraints.

4.2.3 – On Boat Display

Building on lessons learned from previous years, the need was identified for some debugging information to be displayed on the boat. This information included battery voltage, control status of each subsystem, and connectivity of the boat to the wing and base station. A significant design requirement was for the display to be visible in direct sunlight to maximize usefulness in all testing conditions. To meet this requirement, we chose an ePaper display. EPaper display technology does not use a backlight, which results in very low power requirements and excellent visibility in outdoor lighting conditions. The processor at the core of the display was an STM32F103C8 32-bit microcontroller on a small, commercially available development board. This chip features a built-in CAN peripheral to enable interfacing with the NMEA2000 bus, ADCs for measuring battery voltage, and 3.3V logic levels that match those of the ePaper display. To measure battery voltage, a simple voltage divider circuit was developed with using 5.49 $k\Omega$ and 1.78 $k\Omega$ resistors. This provides a maximum voltage of 3.28V to the ADCs at a supply voltage of 13.4V, the voltage of the batteries at full charge (schematic shown in Figure 41. This circuit draws just 1.8 mA of current, and dissipates only 24 mW of power, resulting in very little load on the circuit. The development board draws under 0.5 A of current, and the ePaper display draws 8mA only when it refreshes.

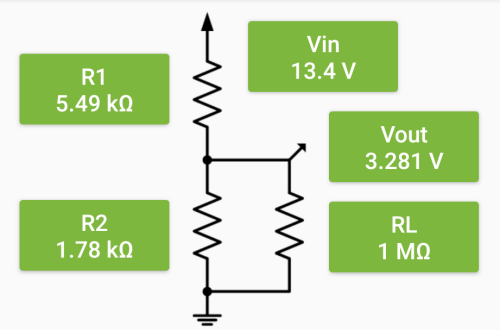

Figure 41: On Board Display Voltage Divider

The display is mounted on the starboard side of the movable ballast bump for good visibility when the boat is at a dock or next to a chase boat.

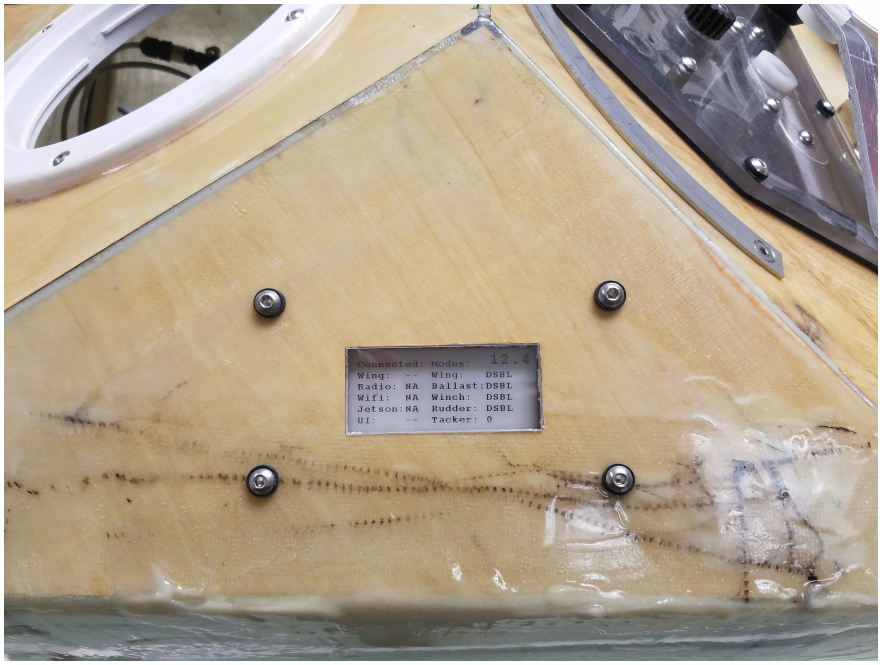

Figure 42: On Board Display Mounted

4.2.4 – Power Distribution

To control the power supply to the boat, a magnetically triggered relay was used. Previous boats used a switch mounted through the hull, but this design suffered from various issues. Waterproof switches rated for our current requirements are difficult to find, are somewhat fragile, and past teams have encountered issues sealing the switch body to the hull. To eliminate the need to pierce the hull, a non-contact solution was desired. To interrupt power, we used a small automotive relay rated for up to 40A, 30% more than the boat is expected to draw. To control this relay, a Melexis US1881LUA latching Hall effect sensor was used as an input to a P-Channel MOSFET which increases the drive current from 50mA to the 200mA required to close the relay coil.

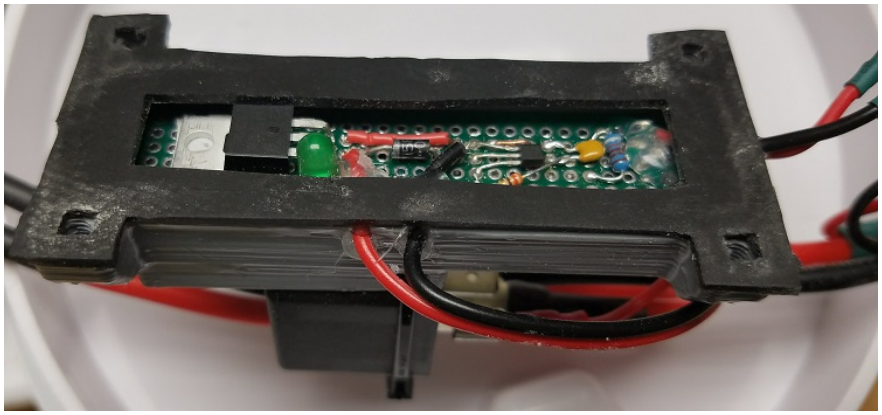

Figure 43: Power Switch

For distribution to the rest of the boat systems, power from the switch enters the fuse box enclosure, where it is split using an automotive fuse holder and bus bar into power leads for the NMEA bus, movable

ballast motor controller, and winch. All of the computing devices on the boat receive their power from the NMEA bus, eliminating the need to run additional power wires to each device.

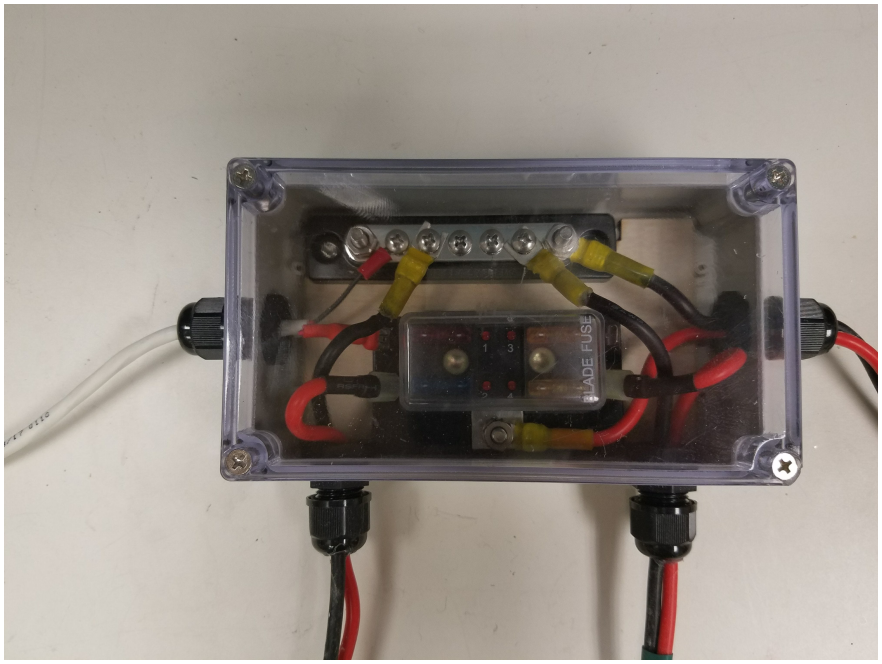

Figure 44: Fuse Box

4.2.5 – Sensors

Position and Wind Sensor

The Airmar 220WX Weatherstation wind sensor provides both true and relative wind speed and direction information. The internal GPS from the Airmar wind sensor provides absolute positioning information.

Orientation/Inertial

The Airmar wind sensor's internal compass and accelerometer was used to estimate the current heading and heel angle of the boat. Although this gives us a reliable estimate of the orientation of the boat, the values provided by this sensor are significantly filtered such that it takes 1-2 seconds for the estimate to converge to the actual value.

Since the movable ballast requires more frequent updates of heel, we added an additional MXC6244AU thermal accelerometer on a breakout board to sense the heel angle of the boat. This connects over I^2C to the movable ballast motor controller, which transmits the heel angle on the CAN bus.

Encoder

To sense the position of the movable ballast arm, a breakout board was developed for a AMS5048 absolute magnetic encoder. The PCB breaks out the Vcc and GND pins to supply power, and I^2C pins for communication. There is a solder jumper on the back to allow configuration for either 5v or 3.3v operation, as well as a power status LED.

4.2.6 – Wireless Communication

In order to view debugging data, set various states, and control the boat remotely, a wireless link needs to be established between the boat and a base station on land. The boat will need to maintain a wireless connection to a control and telemetry station to at least 2 km (approximately 1 nautical mile) line of sight.

This spans the operational area of the competition, including the endurance race, and will allow us to always take control over the boat remotely at any point in time. Several technologies are available for this functionality, such as Bluetooth, WiFi, 4g LTE, and various 900 MHz modulation protocols. The previous boat used a Ubiquiti Bullet M Titanium WiFi radio that is able to transmit at up to 600 mW. With a standard laptop, we observed that the boat was able to maintain connectivity up to about 200m in realistic conditions (observed at the competition at the United States Naval Academy). In order to meet the design specifications, the system either needed to be modified, or a new system needed to be implemented.

High-Power USB Dongle

In order to reduce the system cost, we first attempted to use the existing system with a different WiFi radio setup for the base station. We tested using a Long Range USB WiFi Adapter from Hak5 with the included 5 dbi omni directional antenna. Even though we set the adapter to transmit at its maximum power of 1 W, the boat was still only able to receive beacon frames from the boat to about 250 m. We also tested a 7 dbi patch antenna from Alfa connected to the same USB dongle transmitting at 1 W. With this setup, we were able to receive beacon frames up to about 500m line of sight, but this still does not meet the desired wireless link specifications.

Alternatives

The original system did not come close to the desired specifications for the wireless link, even with some optimizations in the choice of the base station equipment. Since the original WiFi-based system did not look promising, we considered other methods for creating a wireless link between the boat and a base station. With the ubiquity of cell phones, a 4G LTE modem was one of the initial considerations for the wireless link. This would allow us to worry less about antenna optimizations, and recent advancements in technology have enabled significant bandwidth between devices. However, using a 4G LTE modem would restrict the operation of the boat to areas that are covered by cellular towers, which could potentially restrict communications in the Prudence Island test. Further, during previous testing on Lake Quinsigamond (where the competition will be held) cellular connectivity did not appear to be very reliable for the region that we planned on operating in. We chose to not use a 4G LTE modem for these reasons, and only considered point to point wireless technologies.

The point-to-point wireless link technologies that we considered are: WiFi, Bluetooth, Zigbee (IEEE 802.15.4), and various proprietary 900 MHz protocols. Bluetooth was easily eliminated due to the short range limitations of the technology (100m for Class 1 devices) [4]. Previous testing with the existing WiFi setup eliminated the possibility of WiFi being used for the long-range link. Current wireless technologies designed for the Internet of Things such as SigFox, LoRaWAN, etc. were not considered due to their low data rate limitations. Iridium's satellite communication systems were also not considered since the wireless link is not point-to-point, and has low data rate limitations as well.

At the 2017 Sailbot competition, team Aber Sailbot successfully used a pair of XBee radios as their point-to-point wireless link. In addition to the radios, they used an external antenna mounted on the deck of the boat, and were supposedly able to maintain connectivity throughout the 2017 competition (up to approximately 400m). The XBee radios use the Zigbee (IEEE 802.15.4) protocol over a 2.4 GHz carrier, and are rated for up to 250 KBps data transmission rates. These devices interface over a UART serial protocol, and could potentially carry existing ethernet network by using the ser2net protocol and tools with the BeagleBone Black.

Several radios operating on the 900 MHz carrier band were also considered. The 900 MHz ISM band is a more desirable choice due to the better propagation characteristics and distance capabilities compared to the 2.4 GHz ISM band. Devices such as the CDR-915XL from Coyote DataCom [8] and the RFD900 Radio Modem from RF Design [35] offer a bi-directional wireless connection over a 900 MHz carrier signal, and often operate with up to 1W of transmit power. These types of devices tended to offer a transparent serial connection between two devices allowing them to communicate as if they were physically connected. Some have the capability of using frequency hopping techniques such as Direct Sequence Spread Spectrum and

Frequency Hopping Spread Spectrum. These techniques offer better noise immunity and rejection of similar radios operating in the same area. Since the links that competitors are using are unknown, these frequency hopping techniques are desirable to provide a reliable connection.

Digi-Bridge

Ultimately, the XPress Ethernet Wireless Bridge from Digi was selected for use as the long-distance wireless link. This device was selected for several advantages that it had over competing devices. The main advantage of the XPress bridge is that it provides a transparent ethernet connection between two devices. This allows us to directly plug in the radio to the BeagleBone or network router on the boat with minimal configuration, and use existing networking tools and protocols that we are already familiar with and that have already been implemented in previous versions of the control system. The specifications state that the XPress bridge is rated for up to 3.2 km outdoor line of sight with a 2.5 dbi antenna which ideally exceeds our desired specifications [50]. The specifications also state that the bridge uses a Direct Sequence Spread Spectrum modulation, and is capable of up to 935 Kbps data throughput. Although this setup should allow us to maintain connectivity with the boat throughout the operational area, the system is only able to send low throughput data, like simple telemetry streams. When deploying new code to the boat, we observed that a lot of data needs to be transferred, and with the relatively low data throughput of the Xpress bridges, the code upload takes around a minute. There is also a desire to view some of the large data throughput sensors, such as the camera, over a wireless link so that the boat can be debugged on the water. Since the Digi Xpress bridges do not offer this capability, the boat also has a WiFi interface for higher data transfer rates at shorter ranges for easier debugging, testing, and remote code upload.

Wireless Link Testing

In order to validate the claims of the XPress Ethernet Wireless Bridge, we performed several real-world tests to assess the data throughput and link quality. In order for these tests to best reflect the systems capabilities when installed and used on the boat, the tests were conducted between two Xpress devices connected to a BeagleBone Black and a team member's laptop. The program iperf [19] was used to test data throughput and packet transmission quality of the wireless link. A TCP throughput test was used to assess the maximum throughput of the system in the given configuration, and a UDP test at various bit rates was used to assess the number of packets that were dropped at various transmission rates (an assessment of the data transmission quality).

For a control sample, the BeagleBone Black was connected to the laptop directly with an Ethernet cable to determine the maximum throughput and packet transmission quality of the system. To assess the maximum performance of the wireless link, the Xpress devices were connected to both the BeagleBone and the laptop, and a similar test was performed over the wireless link. The Xpress devices were placed 3m apart in the lab in order to reduce other factors influencing the results. Then, the wireless link was assessed in a real-world situation where the Xpress devices were setup on Lake Quinsigamond. The BeagleBone and laptop were separated across the lake at a distance of about 1.5 km. To simulate the wireless link on the boat, the antenna on the Xpress device connected to the BeagleBone was tilted at 25° in several orientations relative to the other antenna. The table below shows the results of all of the tests, and the test on Lake Quinsigamond appears to be the limits of the system with the included 2.1 dbi antennas.

Table 2: Data Throughput and Packet Loss Comparison

Test	Throughput	Packet Loss
Ethernet	94 MBits/s	0.66%
3 m Separation (Lab)	860 KBits/s	0%
38 m Separation (Lab)	860 KBits/s	0%
1.5 km Separation (Lake Quinsigamond)	750 KBits/s	up to 20%
1.5 km Separation, 25° Side-To-Side	500 KBits/s	20%
1.5 km Separation, 25° Away	150-500 KBits/s	30%
1.5 km Separation, 25° Towards	up to 100 KBits/sec	up to 100% packet loss

4.2.7 – Vision

The vision system needs to identify course buoys to round marks more accurately for each course. The vision system should be able to detect buoys moving in and out of the camera frame, recover robustly from occlusions, and report relative locations of all buoys within the field of view from at least 20 meters away. The vision system should also be able to detect boats on potential collision courses and provide relevant course correction data to avoid the impending collisions for the collision avoidance challenge for the ISRC. The locations of the buoys are sampled with a GPS sensor before the event, and were previously used as waypoints to guide the navigation of the boat. However, the location estimates of the buoys and the boat location were limited by the accuracy of the GPS sensor being used. Most commercial and consumer GPS sensors only have an accuracy to within 3 meters in ideal circumstances [46]. This severely limits the navigational accuracy of the boat, such that in non-ideal conditions, the boat may be up to 6 meters away from where it is expecting to navigate to.

The 2017 Sailbot used Raspberry Pi Zero for detecting buoys on the water for the search challenge. The Raspberry Pi Zero was selected due to availability and form factor. Since the Raspberry Pi Zero has a relatively limited processor, it was only able to do simplistic HSV filtering on 320x240 image at 13 fps. This system was only able to detect buoys out to about 3-6 meters, and we wanted to be able to design a more reliable and longer distance detector for buoy tracking.

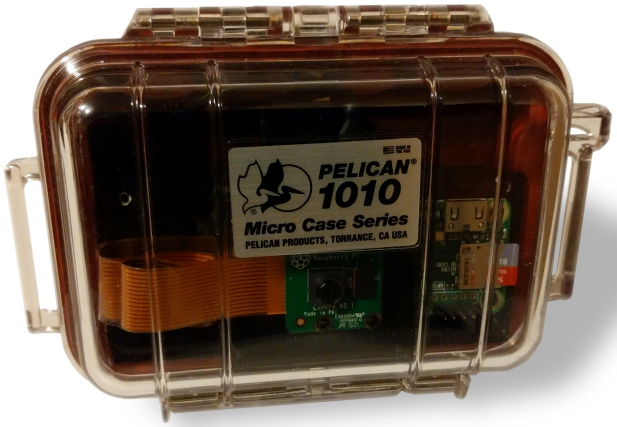

Figure 45: 2017 Vision System

During our research, we found several different methods for detecting arbitrarily shaped objects in a camera's field of view. The most simplistic method is to use a convolutional filter on an intensity image with the shape, size, and values of the filter optimized to find a particular object. Since the buoys will appear to be approximately round, the filter results will be relatively robust to image rotations which will occur from the boat heeling. Different scales of buoys from different distance observations can be compensated for by using image pyramids of the intensity image at different scales. The current state-of-the-art for detecting generic objects though is to use Convolutional Neural Networks trained on a database of reference images [23]. These methods use the full image as the input layer, and break out the image into many regions in the first layer [23]. These regions then go through several steps detecting particular features in each region, and these results are fed to several subsequent layers [23]. The final result is the confidence that the network has for a range of potentially detected objects in the database of reference objects and images, and a proposed bounding box for where each object is in the image [23]. This method has an advantage in that it can be trained on a wide range of input objects and detect several objects at a time in a single image frame. It can also be trained to be robust against lighting, color and scale variances, but needs to have examples of each variance in the database of reference images that it is trained on. The disadvantage to this method however, is that thousands of images are typically needed to train the network weights, and reference data must be

labeled accurately to get useful results. One potential method to side-step the issue of collecting and labeling a large dataset is to use the concept of transfer learning. This method uses a neural network already trained on a large dataset, and attempts to retrain the last few layers of the network with a significantly smaller set of training data [36]. There already exists a large database of labeled images with a wide variety of orientations and examples in the ImageNet database [17], and several neural networks such as AlexNet [24] and YOLO [51] have been successful trained on this database. The ImageNet database has a large collection of different types of boats that could potentially be detected in an image, and we would only need to provide a relatively small set of labeled images to potentially retrain one of the successfully trained networks. Examples of how to do this are available online, such as the tutorial on how to retrain AlexNet on a new set of images using MATLAB [45]. However, due to a lack of available training data from video collected on the boat, these methods were not feasible within the time frame of the project.

The vision system for this year's Sailbot used a NVIDIA TX2 (donated by Professor Michalson) and a wide angle USB camera as seen in figure 46. The camera was selected for its frame rate capabilities of 1024x758 MJPEG images at 60 FPS, and the 170°field of view [16]. This allows the buoy detection algorithms to track buoys over a wide viewing angle was well as further away from the boat than previously. To minimize the the space that the TX2 occupied on the boat, a carrier board was selected to reduce the footprint from the original development board provided with the kit. Several options for a carrier board were considered, including the Orbitty Carrier from ConnectTech, the J120 Carrier from Auvidea, and the J90 Carrier from Auvidea. All 3 options have the same footprint as the TX2 module, but each has several different connectivity features. Ultimately, the J90 carrier was selected due to the built-in CAN transceiver, Ethernet connectivity, USB 3.0, USB 2.0, and built-in IMU [20]. Future projects may also be able to use the dual CSI-2 connectors for higher throughput image frames [20].

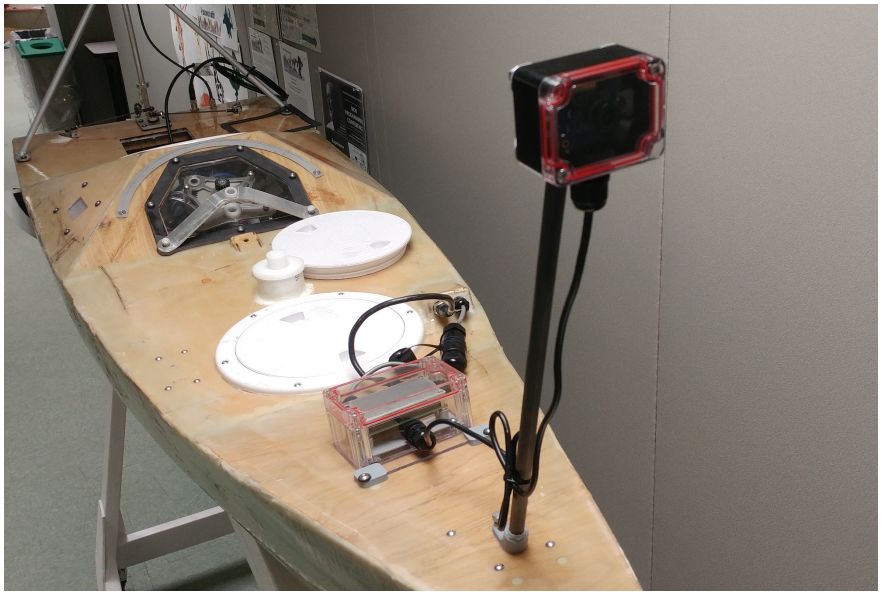

Figure 46: 2018 Vision System

4.2.8 – Buoy Tracking

Due to time limitations, only parts of the buoy tracking were implemented. To improve the navigational accuracy of the sailboat, visual observations of the buoy can be incorporated into the localization system. Since an estimate for the buoy's location is know beforehand, the visual system can sample observations of the buoy while the sailboat is navigating, and continually update the estimated position of the buoy to improve the location accuracy of the buoy. Since the main goal is to simply navigate around the buoys, the relative position between the sailboat and the buoy is more important than a precise location of the buoy in the global coordinate frame. This allows some flexibility in the sampling and estimate updates of the buoy's

location.

Before buoys are localized relative to the sailboat, they must first be detected in an image frame. Our approach used a special color-space transform with a convolution filter to detect brightly colored circular objects in the image that could potentially be buoys. Instead of directly process the RGB data from the sensor, a special color-space transform is used that significantly reduces noise in the resulting image. The current image frame is first converted to the Hue-Saturation-Value color space. This effectively encodes each pixel's value as the color of the pixel, how "colorful" the pixel is, and how bright the pixel is. The hue value for the average water pixel is then subtracted from the hue value of all pixels, and correctly wrapped at the boundaries of the hue values. The final resulting image is then each pixel's shifted hue value multiplied by the intensity and saturation values. This has the effect of highlighting brightly colored areas that are different than the color of the water, and suppressing pixels that tend to be the water or sky as seen in figure 47. After transforming the input image to the new image, a convolution filter is used to find approximately circular shaped objects with a circular kernel. After testing several filter detector methods such as a sum of squared distances detector, zero-mean detector, and normalized cross-correlation, the zero-mean detector gave sufficient performance for the amount of time it took to detect a buoy in each frame. Although normalized cross-correlation gave slightly better results, the frames took between 2-4 times longer to process. Since the results of the correlation are affected by the size of the kernel relative to the object being searched for, an approximate estimate of the distance to the buoy can be detected or filtered. With an estimate of how far the buoy is from the boat, the convolutional filtering can better filter out buoys or other objects outside of a reasonable range.

Figure 47: Colorspace Transformation Results

After detecting potential buoys in each frame, the buoy that the system is tracking needs to be localized relative to the boat. Although we did not have time to further evaluate this system, we designed an algorithm that should be able to track the buoys. Since the zero-mean detector returns some false detections, the estimation methods must be able to account for stochastic sensor data. Two commonly used methods for these types of processes are Kalman filters [22], and particle filters [44]. Kalman filters are able to quickly converge to an estimate of a process value by incorporating measurements and predictions of the current state [22]. Both inputs are used to update the new state of the system, and the Kalman filter maintains an estimate of the error covariances over time [22]. However, Kalman filters are only able to maintain a single estimate of a process value, and cannot handle multiple possible values very well. Particle filters operate in a similar manner to Kalman filters in that they use measurements of the state and predictions of the state to update the new estimate of the system [44]. Particle filters approximate a probability distribution function by maintaining a certain number of samples or "particles" [44]. These particles encode the estimate of the process value in discrete samples, and encode error distributions through weights on each particle [44]. At each state estimate update, the particle filter updates each particle's value from the previous state and any control inputs that have influenced the system. Then, the filter uses the sensor measurements to calculate the probability that a particular particle's value matches what was observed from the sensor. This probability is used as a weighting value for the resampling step. The particles are then resampled with a probability of being selected determined by their weight value, and the same number of particles is sampled for the next state update. This allows the probability distribution function for the state of the system to

approximate any complex probability distribution in a computationally feasible method, and allows for an arbitrary number of possible estimates for the state. This also allows the particle filter to consider two or more possible locations of the buoy, and allows the system to be more robust to sensor noise from false detections.

After potential buoys are found in the image frame, the object that is most likely to be the buoy can be found by comparing the expected location of the buoy from the mean of the particle's positions in the image to all the detected objects in the image. By sorting these objects by the l2 norm from the expected location, the object that is most likely the buoy should be the object with the minimum l2 norm. The most likely candidate can the be reprojected from the camera frame back into the boat's frame by intersecting the detected ray from the camera with the ground plane. The weights of each particle estimate of the buoy's location could then be calculated as the elliptic norm from the projected location (as shown in Figure 48), where the elliptic norm is shown in equation 4.8. Using an elliptic norm allows the error characteristics for the projected angle and the projected distance to be significantly different, since one estimate may be more accurate than the other.

$$||x(t), y(t)||_e = \sqrt{A(t)x(t)^2 + B(t)y(t)^2} \tag{4.8}$$

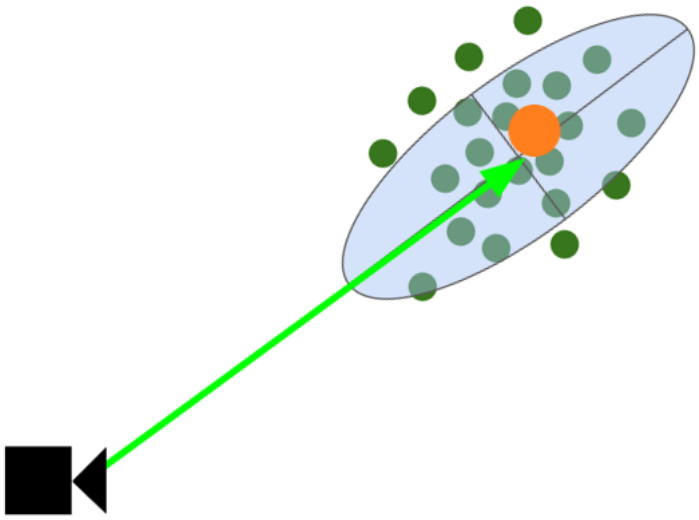

Figure 48: Particle Updates for Buoy Location

5 Testing

5.1 – Full R/C Test

By October 21st, 2017, the boat was ready for a radio controlled test on Lake Quinsigamond. Testing revealed that the winch system quickly wrapped over itself, and needed revision. Additionally, the joint in the movable ballast arm was too flexible, and caused the arm to hit the deck of the boat.

5.2 – Test Stand

To aid in testing and tuning the movable ballast system, a test stand was developed that let us simulate the boat in water. The frame and rotating carriage were constructed from 2x4 lumber, and connected with laser cut gussets. The legs of the stand were designed to allow the keel to clear as the boat heeled, and the stand is mounted on casters to allow for easy movement around the lab space.

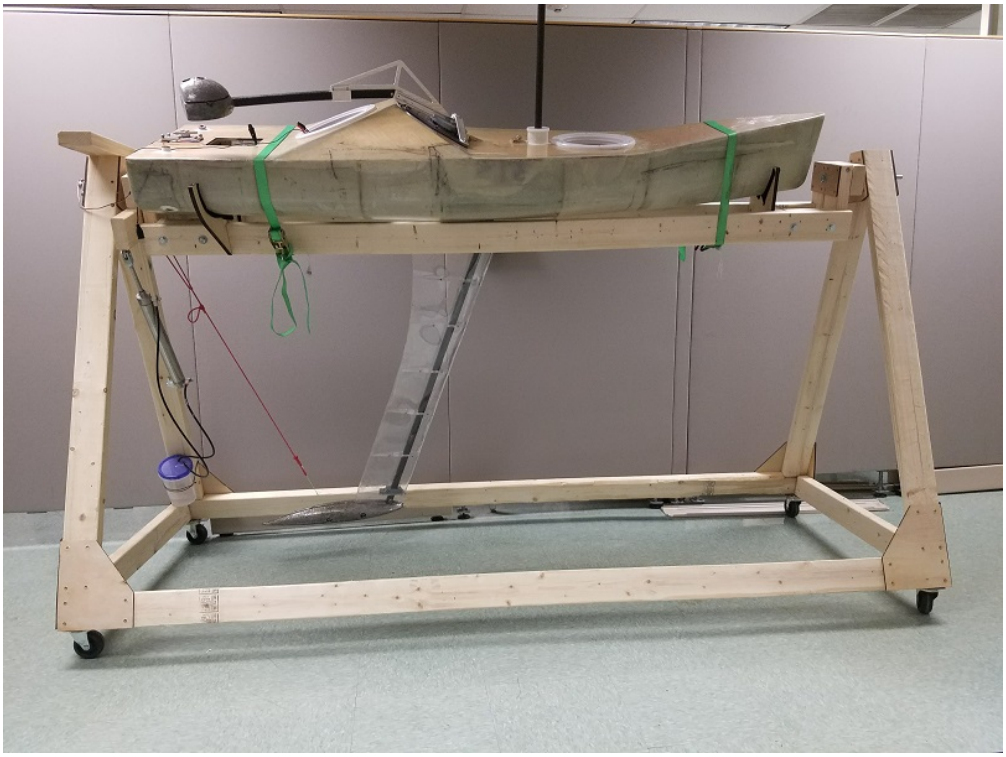

Figure 49: Boat on Test Stand

The carriage pivots in large flanged bearings on each end, and a double acting pneumatic cylinder with flow control valves was installed to provide viscous damping as the boat heels in the stand. One of the pivot shafts has a pocket for a potentiometer shaft to provide "ground truth" heel angles for movable ballast tuning.

5.3 – Endurance Test

The final test for this project was intended to be a circumnavigation of Prudence Island, near Warwick, RI. This approximately eight hour journey would serve as the project's major, final test for the stability and robustness of the mechanical, electrical, and controls systems. However weather postponed earlier testing, and the boat control systems were not sufficiently ready to complete an extended journey autonomously.

6 Communicating About Sailbot

As part of this research project focusing in Professional Writing, I (Travis Norris) created a video to inspire college-aged males to pursue their interests in robotics by demonstrating the iterative design process. Using narrative and discussion as teaching techniques, this video documents the process, challenges, and future implications of creating a robotic sailboat. In this section, I discuss the theories behind narrative and discussion techniques, as well as aspects of documentary films. I also examine two examples of communications about scientific concepts as examples. The first is Dream Machine by Rivka Galchen, a NewYorker article about quantum computing. The second is "Why You Should Put YOUR MASK On First (My Brain Without Oxygen) - Smarter Every Day 157" ("Without Oxygen"), an educational YouTube video by Destin Sandlin on his YouTube channel, SmarterEveryDay. Using interviews with team members and footage of the project, I created a brief documentary that explores the design process in order to de-mystify robotics research and inspire the audience to pursue an interest in robotics.

6.1 – Importance of Communication

Public perception of robotics is generally wary, if not fearful. 89% of European residents believe that "robots are a form of technology that should be closely monitored" and the percentage of people that believe robots are a good thing for society declined between 2012 and 2015 [10]. One large factor in this fear is the belief that robot's take jobs away from people, which was held by 70% of the respondents to that survey. On the other hand, Bernstein et al. [7] theorize that this negative public perception is largely due to portrayal in popular mediums of television and movies. They observe that "regardless of the genre of media, be it comedy, drama, action or horror, robots are shown to be evil". However, increasing interest in robotics can inspire college-aged males to choose a career based on that interest [28].

6.2 – Teaching About Science and Technology

Inspiring others requires educating people about the technology, applications, and scientific concepts behind robotics. However, according to Redish [34], traditional methods of teaching scientific concepts "fail to make an impact on the way a majority of [the] students think about the world." He proposes that students learn by creating mental models based on personal experiences, and that effective teaching must present new mental models that are understandable, plausible, and useful. Vosniadu [47] affirms that "learners possess coherent theories of the world that shape their perceptions of new experiences". In his view, misconceptions are a result of attempts to assimilate contradictory information into an existing mental structure. For robotics, popular culture propagates the mental model of robots as humanoid machines, often with malicious intentions.

Through this project, I attempt to change these mental models using two learning techniques: discussion and narrative. According to the theory of social constructivism, these mental models are often built through interactions with peers, which are an essential part of the learning process [29]. Voss and Sengupta [3] found that students combine their individual points of view to create a joint-understanding that properly explains a specific phenomenon. Similarly, narrative structure can present contradictory mental models in a receivable manner through counterstories. "Counterstories, which challenge the received wisdom ... can open new windows into reality" [9]. Based on Zumbach and Moraz's study [21], linear narrative effectively increases learning over non-linear or encyclopedic information by reducing cognitive load. Counterstories provide an effective method for discussing robotics by demonstrating a narrative that contradicts normal perceptions.

Another method of reducing cognitive load is through the use of multimedia. According to the cognitive theory of multimedia learning [27], humans have limited capacity to process information through auditory and visual channels, and actively engage in the learning process to form mental models. Multimedia structures improve learning by utilizing multiple learning channels to store information in sensory memory, and allowing learners to select relevant information in their working memory. This auditory and verbal information is then integrated with prior-knowledge from long-term memory to yield a new mental model of the topic. Multimedia communication can refer to any type of communication that uses both images and words, but this project focuses on video and film media.

6.3 – Narrative as a Teaching Device

Narrative can similarly be incorporated into educational videos and films. Rather than the theoretical thinking of axioms and predictions, narrative provides a concrete, cause-and-effect interpretation of concepts [39]. Narrative storytelling has many different models, but this study focuses on Freytag's pyramid, and the fantasy-theme model. Freytag's pyramid [13] proposes that narratives follow seven steps:

1. *exposition* - the background, setting and introduction of characters.
2. *inciting incident* - the start of the action that causes the characters to begin a journey.
3. *rising action* - a sequence of events that builds toward a single point of interest.
4. *climax* - the most important moment or turning point of the story.
5. *falling action* - the events that unravel the conflict of the story and maintain suspense.
6. *resolution* - the final resolution of suspense where the characters achieve their goal.
7. *dénouement (epilogue)* - the characters return to a sense of normalcy and conflicts are resolved.

Narratives that follow this pattern build from the exposition through rising action, which builds tension and excitement in the story, and reach their peak in the climax. From there, falling action begins to lead the characters toward a final point of resolution, and remaining questions are answered or explored in the dénouement. Using this structure, I analyzed two examples of scientific narratives. The first is Dream Machine by Rivka Galchen, a NewYorker article about quantum computing. The second is "Why You Should Put YOUR MASK On First (My Brain Without Oxygen) - Smarter Every Day 157" ("Without Oxygen"), an educational YouTube video by Destin Sandlin on his YouTube channel, SmarterEveryDay.

In Without Oxygen, Sandlin begins with exposition about his previous experience with high-altitude training, introduces key characters in the video, and gives an overview of the scientific concept he is explaining, hypoxia. The inciting incident occurs when he begins his high-altitude simulation to deprive his brain of oxygen and show the effects of hypoxia. The rising action builds tension as Sandlin becomes deprived of oxygen, and begins to lose cognitive function. Tension rises as he nears a point of life-threatening hypoxia, and the climax occurs when a NASA flight surgeon intervenes to restore his oxygen supply and prevent any physical harm. Sandlin's speedy return to normal function represents the falling action, and the dénouement occurs as he relates this experiment to the pre-flight safety speech given by flight attendants on commercial airlines which informs you to 'put your own mask on before assisting others'. Sandlin's goal with this narrative is to inspire others to explore the reasoning behind things in their lives in order to better understand the world around them.

The expository themes from Freitag's pyramid are expanded more in the fantasy-theme model [12]. In this narrative structure, 'fantasy' refers not to the popular definition of the term, but instead to the means by which interpretation of communications happen. For instance, interview subjects telling stories of their past experiences, or speaking about future applications of a topic. Fantasy themes tell a story through the experience of a group using three themes: settings, characters, and actions. Setting themes explore the scene of the fantasy, as well as characteristics of that scene. Character themes detail the actors in the story, and provide their traits, motivations, and qualities. Action themes deal with the plotlines that the characters engage in. Fantasies occur only as events other than the current moment, and are often organized in an artistic and non-chaotic fashion. Groups that share fantasies with common settings, characters, and actions create fantasy types, which are mental models of experiences. Combining multiple fantasy types creates a shared interpretation of reality, known as a rhetorical vision. Examples of differing rhetorical visions can be seen in news sources with contrasting political beliefs. Both sources have viewers that see their own source as credible, yet see the other as outlandish. Motives for actions or beliefs based on these sources stem directly from the rhetorical vision of the group.

For example in Dream Machine, Galchen uses these themes to tell the story of quantum computing. The main characters consist of David Deutsch, the 'father' of quantum computing, and Artur Ekert, a former student of his, but Galchen also ties in famous physicists Niels Bohr and Albert Einstein, as well as the fictional character, Sherlock Holmes. The settings range from Deutch's shabby house new Oxford England,

to a quantum computer research lab at Yale university. The fantasies occur as stories about or told by these characters. They include Deutsch and Ekert's initial research together, experiments occurring in the Yale lab, and past arguments between Bohr and Einstein. Deutch's fantasies culminate in his belief in a theory of multiple universes, which many of the other characters disagree with. But Deutch's fantasies that led to the conception of quantum computers are so intertwined with this theory, that to him they are inextricably linked. His rhetorical vision combines these two theories, but other scientists outside of this vision are sceptical.

6.4 – Conversation as a Teaching Device

According to the theory of social constructivism, these mental models are often built through interactions with peers, which are an essential part of the learning process [29]. Voss and Sengupta [3] found that students combine their individual points of view to create a joint-understanding that properly explains a specific phenomenon. To research physics education through multimedia, Muller [29] studied videos with two different teaching styles: one that presented only correct facts, and another that presented common misconceptions of the concepts along with explanations. After collecting the results, Muller found that "students learned better with multimedia when common alternative conceptions were presented in a dialogue format than when only correct information was presented in a lecture style". Despite not actively participating in the discussion of misconceptions, students improved their learning by seeing and hearing the discussions take place. Documentary films typically incorporate discussions like this through interviews.

In Dream Machine, Galchen uses the discussion techniques to encourage various characters to provide feedback about each other's work and to introduce characters and topics. When Galchen introduces the Artur Ekert, Ekert's first quote emphasizes the importance of Deutch's work, saying "David was really the first one who formulated the concept of a quantum computer." He goes on to describe their relationship as researchers at Oxford University, which provides the reader with an introduction to Ekert. Near the end of the article, Galchen again uses discussion to challenge Deutsch's Many Worlds theory by asking one of the Yale researchers, Robert Schoelkopf about the theory. Schloekopf replies that these existential questions are impracticable, and don't need to be part of quantum physics research. Conversely, Deutsch weighs in on Schoelkopf research, and appears fairly unimpressed by the experimental physics.

Sandlin uses conversation as a way to portray the action of his experiment. The beginning and end of Without Oxygen consist primarily of direct address, with Sandlin speaking directly to the audience. However, the central action of the video is portrayed as a conversation between Sandlin and Randy Woodard, an Aerospace Physiology Specialist conducting the experiment. Woodard provides instructions to Sandlin, as well as scientific explanations behind phenomena that are occurring. This discourse engages audience in the action that is occurring, and helps explain the context and implications of the experiment.

6.5 – Video Creation

To create the video, we filmed interviews with team members and project advisors to understand the background, challenges, and future implications of the Sailbot project. We interviewed each person individually and asked about their experiences in sailbot, including previous years. We also asked about their most difficult challenges with the project, and their ideas of possible applications for autonomous sailing. This study was approved by the WPI Institutional Review Board, file number x18-0154.

We filmed each interview from start to finish, and used audio and video excerpts from each as introductions for the interview subject, narrative elements, and technical explanations. Prior to the start of the interview, each interview subject signed a form consenting to participate in the interview, have their responses recorded visually and orally, and have portions of these recordings shared publicly. Interviews lasted 30-60 minutes and consist of introductory questions, technical questions in their field of study, and speculative questions about relevant topics such as the potential impacts of robotics sailing. Before the video was shared publicly, each interviewee had opportunity to view the film and verify that they are accurately portrayed by the video.

Based on the content of these interviews, I created storyboards to layout the narrative structure of the documentary. These storyboards helped shape the flow of ideas and determined the additional footage, explanation, and animation needed for the final video.

During manufacturing and testing of the robot, I recorded footage to use as supplementary imagery, and

documented the successes and failures of the team. One aspect of the project, the movable ballast, emerged as the most engaging narrative option. Because of several failed design iterations and an interesting technical concept, I chose to focus the documentary on the movable ballast by selecting footage and interview clips about the movable ballast. When editing, I chose specific discussion points from the interviews and paired them with interesting video I had taken. I added further context with narrated explanations, animated demonstrations, and stock footage. The resulting documentary consisted of 10 key elements:

1. *Premise*- The premise introduces the common misconception that robots are only humanoid machines and gives the audience a familiar starting point to progress from. In the premise, I use stock footage of humanoid robots as well as robots from popular culture to provide a familiar starting place for the video.

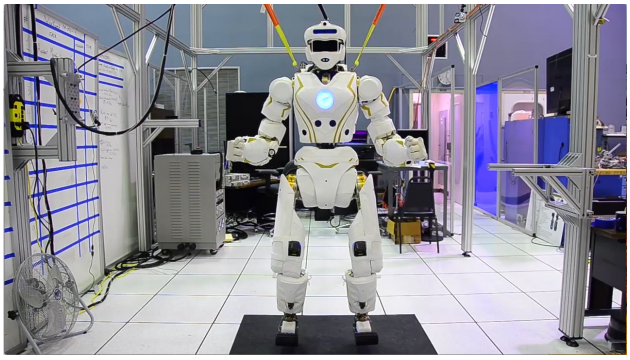

Figure 50: A Humanoid Valkyrie Robot Developed by NASA

2. *Disruption*- The disruption shows examples of non-humanoid robots in a variety of industries to show the diversity of robotics. I chose to show industrial robots in manufacturing and consumer robots in homes, because each demonstrates a very different side of robotics. This section also sets up the research and competition aspects of the robotics industry as an introduction to the Sailbot project. I chose to use footage from the DARPA robotics challenge, which shows a robot driving a car, and from Battlebots, which shows a competitions purely for entertainment. Some viewers may also be familiar with the Battlebots TV show, further solidifying the premise.

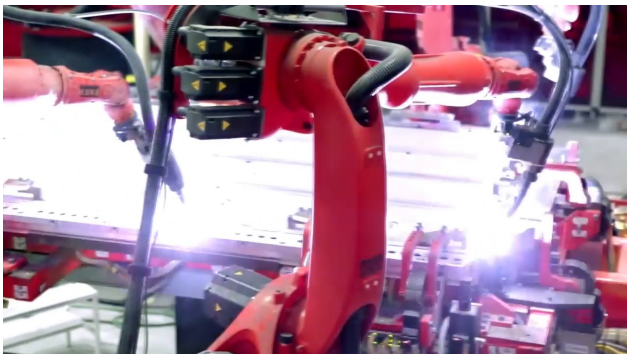

Figure 51: A Kuka Robot Arm Welding a Car Body

3. *Setting*- The setting establishes the Sailbot competition as the subject area and familiarizes the audience with some of the challenges of the event. I chose to use footage of multiple boats to demonstrate the competitive aspect, and footage of the WPI team to transition into their introductions.

Figure 52: The 2016 Sailbot Competition

4. *Introductions*- In the introductions, the audience meets the main characters and establishes their expertise in robotics. These include Jordan Burklund, Hans Johnson, and Professor Ken Stafford. As veterans of the sailbot project and robotics engineers, they are well suited to discuss the technical aspects of sailbot. I chose to start with Professor Stafford's interview, because he describes the competition well, and talks about the students he works with. This provides a smooth transition into interviews with Jordan and Hans to discuss the background.

Figure 53: Professor Ken Stafford Discussing Sailbot

5. *Background*- The background consists of interviews from the previous Sailbot projects. The characters explain some of the successes and failures of previous years, and the lessons learned from those experiences. This sections serves as a precedent for the complications later in the video. This section consists mostly of footage of Jordan and Hans working overlaid with interview audio with each of them. Because the information is coming from the team members and not a narrator, the audience can more easily connect with the characters in the video.

Figure 54: Jordan Describing Past Sailbot Attempts

6. *Exposition*- In the exposition, I used animation and interviews to explain some of the scientific concepts behind the movable ballast design and to begin the narrative for the video. The exposition helps introduce some of the sailing terminology commonly used by the characters. I interspersed footage of real sailboats with the animation to help the audience understand how the robot emulates real human actions. By describing the technical concepts, the video also provides motivations for this system and how it can be useful when sailing.

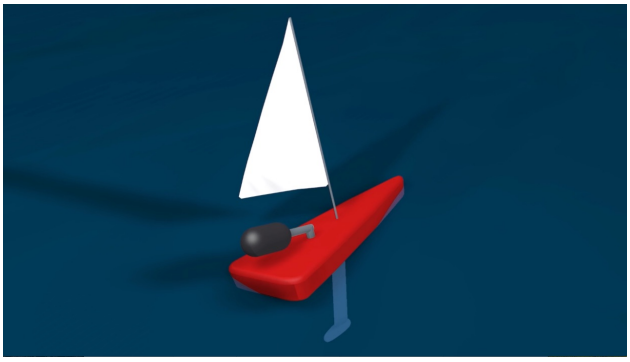

Figure 55: An Animated Sailboat Demonstrating Heel

7. *Rising Action*- During the rising action, I show the team designing and manufacturing the movable ballast system. This includes a walkthrough of the 3D model of the system, and a montage of manufacturing different components. This provides a technical explanation for anyone who is curious about the designs, as well as demonstrates the amount of work required to design this system. This raises the stakes for the upcoming conflict.

Figure 56: Hans Manufacturing Components of Sailbot

8. *complication*- The complication occurs when the original design for the movable ballast doesn't work, and the team needs to come up with a better solution. This demonstrates the iterative design process used in the Sailbot project as well as shows the imperfections of engineering design. These two concepts can help make engineering more human-oriented and attainable for the audience.

Figure 57: Travis Describing the Issues with the Design

9. *climax*- The climax resolves the compicaltions of the movable ballast and demonstrates it functioning on the boat. This section wraps up the technical background by showing a real example of the theoretical concept and resolves the narrative arc of the team's efforts. Along with footage of the system working, I included footage of the team smiling, to show the audience the excitement in a working system. This improves the payoff for the audience by showing the characters' success.

Figure 58: Hans Assembling the Movable Ballast for Testing

10. *Resolution*- Finally, the resolution explores the future implications of robotic sailing, such as ocean research or defense, and emphasizes the benefits of robotics research. This section uses more interviews with Professor Stafford and stock footage of professional companies to emphasize the larger impact of this research. This is intended to inspire the audience to realize that robotics research is providing benefits to society, and may be something they would like to pursue.

Figure 59: An Autonomous Boat Made by Saildrone

6.6 – Video Testing

To develop content for the video, I used 3 different methods to facilitate better communication. I used storyboards to develop the narrative structure, user testing to identify points of confusion, and focus groups to determine where additional content was needed. This testing was conducted with approval from the WPI IRB, File 18-0154.

To create the storyboards, I used a presentation software to develop basic visual layouts for each section, and wrote a script for introductory and explanatory narrations. Each slide consisted of very basic visuals with a few sentences to provide the narration. I also laid out the framework of the narrative structure to determine the footage needed for the story and types of questions to ask in interviews. For the narrative storyboards, I included hypothetical quotes from the interviewees to better inform the story. I practiced reading through the script, and timed myself reading all of the narration to get a better understanding of the video pacing. A draft of these storyboards is located in Appendix F

Once the storyboards were created, I tested them with 4 potential audience members to determine points of confusion or areas that needed more explanation. I then used the feedback to revise the storyboards and the video itself. I selected audience members through convenience sampling, and only chose participants who were unfamiliar with the Sailbot project. First, I explained the purpose of my research for making a documentary video, and allowed the participants to ask questions about the project. Then, I had each

participant read through the narration script and view the storyboards at their own pace, and then asked them to point out areas of confusion. I specifically asked questions such as 'Which sections, if any, of the story were confusing?' and 'Is there any part of the project you would like to know more about?'. In addition to these questions, I also noted anywhere that the participants asked questions during the initial reading. The discussions lasted 10-15 minutes. I compiled the notes from these evaluations and selected one area to improve based on the most common comments.

After the video was created, I conducted focus groups to receive feedback on the overall quality, as well as areas that needed more information. I conducted three, 30-minute focus groups, which consisted of three audience members viewing the video together, then discussing their likes, dislikes, and areas of improvement. The audience members were chosen through convenience sampling, and each arrived at their own convenience. Once everyone had arrived, I explained the purpose of the focus group, and allowed any participant to ask questions about the study. Then, all participants viewed the together video on a projector screen with a front-of-house audio system. At the conclusion of the video, I asked them to discuss among themselves their initial thoughts and comments. I then asked a series of questions about their understanding and enjoyment of the video, such as 'what did you particularly like or dislike about the video?' or 'In your own words, what was the overall message of the video?'. The viewing lasted approximately 10 minutes with the discussion lasting, on average, 20 minutes. The full list of questions is available in Appendix G.

These three testing devices helped shape the video and identify areas of improvement. The storyboards helped develop the narrative of the video, while the user testing identified a disconnect in the Premise. Finally the focus groups showed a greater interest in the setting and background, particularly relating to the Sailbot competition.

I used the lessons learned from storyboarding to help shape the interview question for the video, and to direct my attention toward finding a narrative. Originally, the video focused on several issues and challenges with the Sailbot project. Storyboarding helped display the disorganized flow of this structure, and helped me condense the narrative into a single plot line. The storyboards also served as a guide for pacing and visual reference during the editing process.

The user testing helped me identify a disconnect between the premise and the introduction to Sailbot. In early drafts, the storyboards transitioned from humanoid robots to the Sailbot competition without much context. Of the four user testing participants, two mentioned that the connection between those two ideas seemed lacking in the video. Based on that feedback, I added background to demonstrate the diversity of robotics, from industrial automation to home companions.This transition flows more smoothly, and prevents the audience from feeling lost.

The focus groups were effective in pointing out several technical flaws in the video. Firstly, some of the audio from interviews was excessively quiet, making it difficult to hear from the audience perspective. Additionally, one participant noted a few choppy transitions and visual mistakes that required minor editing shifts to remedy.

Finally, three of the nine focus group participants specifically mentioned a desire to learn more about the Sailbot competition itself. They wanted to know the types of challenges required for competition, as well as get to see other teams from the event. Unfortunately, it was not possible to interview any other event participants in the available time frame. However, I added narration and video footage to further explain the Sailbot competition, particularly obstacle avoidance challenge.

6.7 – Conclusion

Through this project, I discovered the effectiveness of narrative storytelling in communicating about science and technology, as well as the structure of short-form documentary for the same application. One major challenge posed by this format is the large quantity of unused and excess footage. Because it is difficult to know the narrative of the documentary before speaking with the characters and experts, documentary-style films require the director to film very broad topics in the beginning of the process, and narrow down the scope of interview questions and video footage as the project continues. Additionally, various technical topics come with their own jargon, scientific concepts, and public predispositions toward them.

Documentary formats can be used to inspire people across various fields and interests. Future research should look at the effectiveness of similar methods in various science and technology fields. Particularly, research could examine how different projects or topics would require varying levels of background and

exposition. One such topic could be the public acceptance of Genetically Modified Organisms (GMOs). Alternatively, research could apply this same narrative style to non-technical communications, and explore the differences for communicating about artistic endeavors.

Overall, narrative storytelling and discussion-based documentaries provide effective tools for communicating about science and technology. This project analyzed the elements required to create an effective documentary narrative, and applied that structure to create an inspirational video about the Sailbot project. By revising and testing the story and final video, I was able to develop a short-form documentary with the purpose of inspiring audience members to pursue an interest in robotics.

7 Recommendations for Future Work

This section covers the areas of future work we recommend, particularly to improve the robustness of Sailbot, continue progress on existing goals, and experiment with new designs. This section covers mechanical recommendations in keel design, weight reduction, winch design and ballast construction. Additionally we provide recommendation for the motor controllers and control system for the boat.

7.1 – Mechanical Recommendations

This section explores improvements to mechanical designs that have the potential to improve the the performance of Sailbot.

7.1.1 – Keel Design

The keel design could be improved to create a more efficient, lighter, and smoother keel. To limit the scope of this project, little aerodynamic analysis was done on the keel shape, instead relying on design examples to provide an effective solution. Future researchers could experiment with various hydrofoil shapes, sweep angles, and surface areas to provide more efficient lift and reduce drag. Additionally, future research may explore various construction techniques to produce a lighter keel structure without compromising stiffness.

7.1.2 – Winch Design

The winch design effectively prevents tangling in the mainsheet, but there is still significant room for improvement. The design is quite heavy, with a large number of metal parts. Additionally, the design is quite sensitive to sheet diameter and stiffness, requiring fine tuning for each new type of sheet. Spring loading the rollers may be a solution, as well as exploring other design concepts. Improving the robustness of the winch design will increase the long-term reliability of the Sailbot when using the cloth sail.

7.1.3 – Ballast Construction

The movable ballast underwent several design revisions before the final iteration this year. Due the high dynamic loads and potential stress concentrations, the whole system should be examined thoroughly for signs of wear or failure. Particularly, the polycarbonate sheet that attaches to the deck may experience cracking or fatigue from the stresses, and will likely need to be replaced in the future.

7.1.4 – Wingsail

While this year's wing sail met the goals of a lighter mechanical system and more robust electrical system, the lighter system came at the cost of flexibility and mechanical robustness. In moderate winds, the carbon fiber mast at the core of the wing sail bends, and the tip of the wing sail visibly deflects up to an estimated 0.30 m. Additionally, the lightweight balsa foil sections are fragile, and susceptible to damage during transportation and rigging.

7.1.5 – Weight Reduction

Though progress has been made in reducing the overall weight of the boat, further work could explore ways to further reduce weight, particularly in the keel structure, cloth sail mast, and various mechanisms. Despite this year's team choosing to reduce the length of the keel, a longer keel would require less ballast to provide the same righting moment.

7.2 – Control Recommendations

This section explores some of the possible areas for additional development in the control of Sailbot.

7.2.1 – Motor Controllers

While the motor controllers can successfully read CAN messages and output power, they exhibit errors on initial startup and when communicating with sensors. The ballast motor controller specifically does not

properly initialize when the boat is turned on, and must be manually restarted. Additionally, after some time, it appears to lose I^2C connection with the inclinometer and encoder. While workarounds are in place to allow the boat to operate, future research should prioritize finding the source of these motor controller issues. The addition of a CAN based bootloader could also improve the process of updating software on the motor controllers. Currently the motor controller must be removed from its case and the programming headers plugged into a dedicated programming device. By implementing a CAN based bootloader such as OpenBLT [11], code for the motor controllers can be uploaded in the field through the BeagleBone Black or other Linux based processor connected to the CAN bus.

Small pitch headers for sensors and programming were initially selected, but proved to be difficult to work with in practice. These headers were selected to reduce the footprint of the motor controller, but in the end it would have been more beneficial to work with more standard sized headers, such as 2.54mm pitch headers that are common with hobbyist electronics. These headers are easier to interface with without fine soldering, and low-cost tools are available to make custom wiring harnesses.

7.2.2 – Ballast Control

The complex dynamics of the movable ballast provide and interesting challenge for control. While the current system can induce and maintain heel angles, it is by no means optimal. Future research could explore optimization of the ballast control algorithms to reduce response time, decrease power consumption, or increase responsiveness to minor disturbances such as changing winds. The ballast could even switch between several different control plans to meet the needs for endurance, speed, or stability.

7.2.3 – Vision System

The vision system has been developed enough to identify buoys within video footage, but has not yet been implemented to determine the buoy position relative to the boat. Future research could implement the suggested algorithms to localize the buoys, and compare them to expected GPS coordinates. Implementing this system will allow the path planner to more accurately and efficiently determine routes for rounding buoys. Additionally, the object detection methods could be expanded to identify obstacles and other hazards to help the boat in the obstacle avoidance challenge.

Bibliography

[1] *AISI 4140 Steel*. URL: http://www.matweb.com/search/DataSheet.aspx?MatGUID=8b43d8b59e4140b88ef666336ba73 7B%5C&%7Dckck=1 (visited on 03/30/2018).

[2] *Aluminum 7075-T6; 7075-T651*. URL: http://www.matweb.com/search/DataSheet.aspx?MatGUID=4f19a42be94546b686bbf43f79c51b7d%7B%5C&%7Dckck=1 (visited on 03/30/2018).

[3] Pratim Sengupta Amy Voss Farris. "Perspectival Computational Thinking for Learning Physics A Case Study of Collaborative Agent-based Modeling ". In: (). URL: https://arxiv.org/pdf/1403.3790.pdf (visited on 03/30/2018).

[4] *Bluetooth Power Classes: Class 1, 2 and 3*. URL: http://bluetoothinsight.blogspot.com/2008/01/bluetooth-power-classes.html (visited on 03/30/2018).

[5] Boat Indiana. *Parts of a Sailboat*. 2017. URL: https://www.boat-ed.com/images/drawings/sailboat.jpg.

[6] *CAN in Automation (CiA): Controller Area Network (CAN)*. URL: https://www.can-cia.org/ (visited on 03/30/2018).

[7] *Consumer Robotics State of the Industry and Public Opinion*. URL: https://web.wpi.edu/Pubs/E-project/Available/E-project-050510-125007/unrestricted/Consumer_Robotics_-_State_of_the_Industry_and_Public_Opinion.pdf (visited on 03/30/2018).

[8] *Coyote DataCom OEM Module: CDR-915XL*. URL: http://www.coyotedatacom.com/products/oem%7B%5C_%7Dradio/CDR915XL.htm (visited on 03/30/2018).

[9] Richard Delgado. "Legal Storytelling". In: (). URL: http://www.jstor.org/stable/1289308 (visited on 03/30/2018).

[10] *European Commission: Eurobarometer 427 Autonomous systems*. URL: http://ec.europa.eu/commfrontoffice/publicopinion/archives/ebs/ebs_427_en.pdf (visited on 03/30/2018).

[11] Feaser. *Open Source Bootloader Tool*. URL: https://www.feaser.com/openblt/doku.php?id=homepage.

[12] Sonja K Foss. *Rhetorical criticism: Exploration and practice*. Waveland Press, 2017.

[13] Gustav Freytag. *Freytag's technique of the drama: an exposition of dramatic composition and art*. Scholarly Press, 1896.

[14] *GNU Arm Embedded Toolchain in Launchpad*. URL: https://launchpad.net/gcc-arm-embedded (visited on 03/30/2018).

[15] *Harken Self Tailing Winch*. URL: http://www.harken.com/uploadedImages/Products/fb027491-2059-4b96-8bf6-02e06d49d25d%7B%5C_%7Dlarge.png (visited on 03/30/2018).

[16] *High-Speed 120fps USB Camera Module*. URL: http://www.elpcctv.com/highspeed-120fps-usb-camera-module-usb20-ov2710-color-sensor-mjpeg-format-36mm-lens-p-224.html (visited on 02/24/2018).

[17] *ImageNet*. URL: http://www.image-net.org/ (visited on 03/30/2018).

[18] *International Robotic Sailing Competition*. 2017. URL: http://sailbot.org.

[19] *iPerf - The TCP, UDP and SCTP network bandwidth measurement tool*. URL: https://iperf.fr/ (visited on 03/30/2018).

[20] *J90 compact carrier board for TX1/TX2*. URL: https://auvidea.com/product/70760/ (visited on 01/31/2018).

[21] Maryam Mohraz Joerg Zumbach. "Cognitive load in hypermedia reading comprehension Influence of text type and linearity". In: (). URL: https://doi.org/10.1016/j.chb.2007.02.015 (visited on 03/30/2018).

[22] Rudolph Emil Kalman. "A New Approach to Linear Filtering and Prediction Problems". In: *Transactions of the ASME–Journal of Basic Engineering* 82.Series D (1960), pp. 35–45.

[23] Ujjwal Karn. *An Intuitive Explaination of Convolutional Neural Networks*. URL: https://ujjwalkarn.me/2016/08/11/intuitive-explanation-convnets/.

[24] Alex Krizhevsky, Ilya Sutskever, and Geoffrey E Hinton. "ImageNet Classification with Deep Convolutional Neural Networks". In: (). URL: https://papers.nips.cc/paper/4824-imagenet-classification-with-deep-convolutional-neural-networks.pdf.

[25] *Maretron - NMEA 2000 Cable and Connectors*. URL: https://www.maretron.com/products/cabling.php (visited on 03/30/2018).

[26] *Maritime Security Solution Provides Protection Security and Intelligent Surveillance of the Ocean*. URL: http://www.oceanaero.us/defense-Maritime-Security-solution (visited on 03/30/2018).

[27] Richard E Mayer. *The Cambridge handbook of multimedia learning*. Cambridge University Press, 2005.

[28] Carolyn Morgan, James D Isaac, and Carol Sansone. "The role of interest in understanding the career choices of female and male college students". In: *Sex Roles* 44.5-6 (2001), pp. 295–320.

[29] Derek Alexander Muller. *Designing Effective Multimedia for Physics Education*. Tech. rep. URL: http://www.physics.usyd.edu.au/super/theses/PhD%28Muller%29.pdf (visited on 03/30/2018).

[30] *Official Repository of WPILibJ and WPILibC*. URL: https://github.com/wpilibsuite/allwpilib.

[31] *Olin Winch Layout*. URL: https://www.rmgsailwinch.com.au/rmg/product%7B%5C_%7Dimages/uploaded%7B%5C_%7Dimages/stRper1.jpg (visited on 03/30/2018).

[32] *Overview of brushed DC motor program — maxon motor*. URL: https://www.maxonmotorusa.com/maxon/view/content/brushed-dc-motors (visited on 03/30/2018).

[33] Frédéric Plumet et al. "Toward an Autonomous Sailing Boat 2015 Romero". In: 40.2 (2015), pp. 397–407.

[34] Edward F. Redish. "Implications of Cognitive Studies for Teaching Physics". In: ().

[35] "RFD900 Radio Modem Data Sheet RFD900 Product Specifications and Performance RFD900 Configuration RFD900 Modem Tools User Manual". In: (2013). URL: http://files.rfdesign.com.au/Files/documents/RFD900%20DataSheet.pdf.

[36] Sebastian Ruder. *No Title*. URL: http://ruder.io/transfer-learning/.

[37] Hadi Saoud et al. "Routing and course control of an autonomous sailboat". In: *2015 European Conference on Mobile Robots, ECMR 2015 - Proceedings* (2015), pp. 3–8. DOI: 10.1109/ECMR.2015.7324218.

[38] *Sourcery CodeBench Lite Edition including ARM GCC IDE - Mentor Graphics*. URL: https://www.mentor.com/embedded-software/sourcery-tools/sourcery-codebench/editions/lite-edition/ (visited on 03/30/2018).

[39] Russell Stannard. "Communicating physics through story". In: *Physics education* 36.1 (2001), p. 30.

[40] "STEEL PRODUCT MANUAL". In: (). URL: http://www.vanguardsteelvancouver.com/Publish/Images/Cat/Vanguard%7B%5C_%7DSteel%7B%5C_%7DProduct%7B%5C_%7DManual%7B%5C_%7DFull/Vanguard%7B%5C_%7DSteel%7B%5C_%7DProduct%7B%5C_%7DManual.pdf.

[41] *STM32F042K6 - Mainstream ARM Cortex-M0 USB line MCU with 32 Kbytes Flash, 48 MHz CPU, USB, CAN and CEC functions - STMicroelectronics*. URL: http://www.st.com/en/microcontrollers/stm32f042k6.html (visited on 03/30/2018).

[42] *Summer of Sailing Drones*. URL: https://research.noaa.gov/News/NewsArchive/LatestNews/TabId/684/ArtMID/1768/ArticleID/12205/Summer-of-sailing-drones.aspx (visited on 03/30/2018).

[43] *Talon SRX - VEX Robotics*. URL: https://www.vexrobotics.com/217-8080.html (visited on 03/30/2018).

[44] Sebastian Thrun. "Particle filters in robotics". In: *Proceedings of the Eighteenth conference on Uncertainty in artificial intelligence*. Morgan Kaufmann Publishers Inc. 2002, pp. 511–518.

[45] *Transfer Learning Using AlexNet - MATLAB & Simulink*. URL: https://www.mathworks.com/help/nnet/examples/transfer-learning-using-alexnet.html?s%7B%5C_%7Dtid=gn%7B%5C_%7Dloc%7B%5C_%7Ddrop (visited on 03/30/2018).

[46] U.S. Department of Defense. *Global Positioning System Standard Positioning Service Performance Standard*. 2008. URL: https://www.gps.gov/technical/ps/2008-SPS-performance-standard.pdf.

[47] Stella Vosniadou. "Capturing and modeling the process of conceptual change". In: (). URL: https://doi.org/10.1016/0959-4752(94)90018-3 (visited on 03/30/2018).

[48] *Weather History for Worcester, MA — Weather Underground*. URL: https://www.wunderground.com/history/airport/KORH/2017/6/12/MonthlyHistory.html?req%7B%5C_%7Dcity=%7B%5C&%7Dreq%7B%5C_%7Dstate=%7B%5C&%7Dreq%7B%5C_%7Dstatename=%7B%5C&%7Dreqdb.zip=%7B%5C&%7Dreqdb.magic=%7B%5C&%7Dreqdb.wmo= (visited on 03/30/2018).

[49] *Worcester Polytechnic Institute Sailbot Autonomous Robotic Sailboat*. Tech. rep. URL: http://www.wpi.edu/academics/ugradstudies/project-learning.html.

[50] *XPress Ethernet Bridge Product Detail - Digi International*. URL: https://www.digi.com/support/productdetail?pid=4465%7B%5C&%7Dtype=documentation%7B%5C#%7Dspecifications (visited on 03/30/2018).

[51] *YOLO: Real-Time Object Detection*. URL: https://pjreddie.com/darknet/yolo/ (visited on 03/30/2018).

Appendices

A Manufacturing

This appendix covers details of the manufacturing processes used in the construction of the boat and its components.

Hull

The hull of the boat is constructed from fiberglass and reinforced with wood ribs. The hull is composed of four layers of 6oz fiberglass cloth, with the second and fourth layers laid 45 degrees off-axis to improve stiffness. To create the hull shape, we constructed a male plug from expanded polystyrene insulation foam and laser cut wooden cross sections. We hand-sanded the foam between the cross sections, and smoothed the surface with Bondo. The fiberglass was then laid over the form, and vacuum bagged to remove air bubbles and excess resin. The bow and transom are reinforced with additional fiberglass layers to maintain strength during normal, low speed collisions. The plywood ribs are attached to the hull with fiberglass strips and fillets made from structural adhesive filler. The size of the plywood ribs was the constraining factor on the beam of the boat, as the laser cutter at WPI has a maximum cutting dimension of approximately 60cm.

The deck of the boat was constructed from laser cut plywood, sandwiched between layers of fiberglass. The seams were reinforced with resin and West Systems 404 High Density Adhesive filler, and have additional layers of fiberglass for strength. Hatches forward of the mast and aft of the movable ballast bump allow access to the internals of the boat, for maintenance of the electronics and installation of batteries.

Winch

The powered drum was constructed in two parts, an inner core that was pressed into an outer shell. This allowed the drum to be mostly hollow to save weight. To interface with the motor, the turned center core was mounted in a mill and the mating profile for the motor shaft was machined into it. This allowed us to gradually adjust the mating profile to achieve a tight fit with minimal lash.

Keel

The keel was originally designed as a square carbon fiber core, with a polycarbonate skin supported by PETG ribs. While this was functional, excessive deflection required us to remanufacture it. The second iteration used laser-cut acrylic ribs and a fiberglass skin. The fiberglass was pre-wetted on a table, and then draped over the ribs to form the outer skin. Filler was added to smooth the surface, and a second layer of fiberglass reinforced the skin and sealed the trailing edge more effectively.

The major constraint of the design was the cost of the carbon fiber tubing. We used a roll wrapped carbon fiber tube with a 1.588 mm (1/16 in) wall. Empirical testing revealed more deflection than the Finite Element Analysis predicted, particularly in torsion. To stiffen the keel, we wrapped the carbon tube in fiberglass and added a section of a carbon fiber mast with spacers in-between. This reinforcement, along with the fiberglass skin, eliminated almost all deflection from the keel. However, the increased stress concentration at the hull connection caused the carbon fiber to break. To remedy this, we machined a 20 cm aluminum insert and attached it inside the tube with epoxy.

The keel bulb is made from cast lead, covered in epoxy and bolted to a stainless steel support. We 3D printed forms for the bulb in two halves, and used body filler to provide a smoother finish. We then made plaster molds of these forms, and baked them in an oven for several hours to remove any moisture. At a local industrial makerspace, we cast the bulbs, and machined a channel for the support. We then coated the bulb in epoxy resin and fiberglass filler to prevent contamination, and attached it to the support with through bolts. This support bolts into the end of the keel.

To attach the keel to the hull, we used the carbon fiber tubing as a mold to make two fiberglass tubes. These tubes were then placed inside the hull and reinforced with fiberglass and plywood. A thumbscrew above the deck threads into a stainless steel insert in the carbon fiber tube and secures the keel to the hull. This design allows the keel to be securely attached to the hull and removed without the use of any tools.

Rudders

The rudders are constructed of three 3D printed segments and an embedded aluminum drive shaft, covered in a single layer of fiberglass and resin. The 3D printed sections were printed out of PLA with a single perimeter and low infill, as their primary purpose was to provide the shape around which the fiberglass could be formed. The fiberglass provides strength and rigidity, and was sanded smooth to minimize drag. The aluminum shaft has a small plate welded into the end, which fits in a pocket between two of the printed segments. This provides the power transfer between the shaft and plastic segments. The assembly of these parts is pictured in Figure 14.

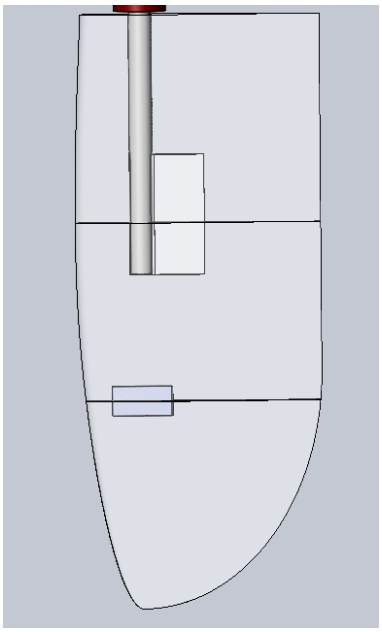

Figure 60: Rudder Composition

Movable Ballast

Movable ballast parts were manufactured by multiple sources using multiple processes. The lead counterweight was cast using the same process as the keel bulb. The polycarbonate mounting plate was cut on a waterjet, and then the pocket for the shaft seal was CNC milled. The shaft pivot plate, retention strap, and gearbox plates were laser cut from aluminum, and the remainder of the parts were machined.

In particular, the movable ballast arm presented a significant machining challenge, due to the complexity of the finished part. It required four setups, each with different fixturing, and a total of 10 tools to complete (including hand tapping). A strong recommendation for future versions of this part would be to redesign it with more attention paid to its manufacturability.

B Mainsail Load Calculation

Based on `http://www.harken.com/MainsheetLoading/`

$$ML = \frac{E^2 * P^2 * 0.02104 * V^2}{\sqrt[2]{P^2 + E^2} * (E - X)} \tag{B.1}$$

E (foot length, m) = 1.2
P (luff length, m) = 3
V (wind speed, kt) = 8 (typical for competition/testing conditions)
X (distance from aft end of boom to mainsheet attachment, m) = 0
ML = 5 kg = 49.1N
While it is unclear why they use kilograms for measuring force, a conversion of 9.81 N/kg was used to convert to force

C Winch Motor Data

Speed (rpm)	Torque (Nm)	Current (A)	Power (wt)	Efficiency	Heat (wt)
0	5.65	12	0	0%	144
6	5.27	11.3	3.2	2%	133
11	4.9	10.6	5.9	5%	121
17	4.52	9.9	8.1	7%	111
23	4.14	9.2	9.9	9%	101
29	3.77	8.5	11.3	11%	91
34	3.39	7.8	12.2	13%	82
40	3.01	7.1	12.7	15%	73
46	2.64	6.5	12.7	16%	65
52	2.26	5.8	12.2	18%	57
57	1.88	5.1	11.3	19%	49
63	1.51	4.4	9.9	19%	43
69	1.13	3.7	8.1	18%	36
75	0.75	3	5.9	16%	30
80	0.38	2.3	3.2	12%	24
86	0	1.6	0	0%	19

D Motor Controller PCB Design

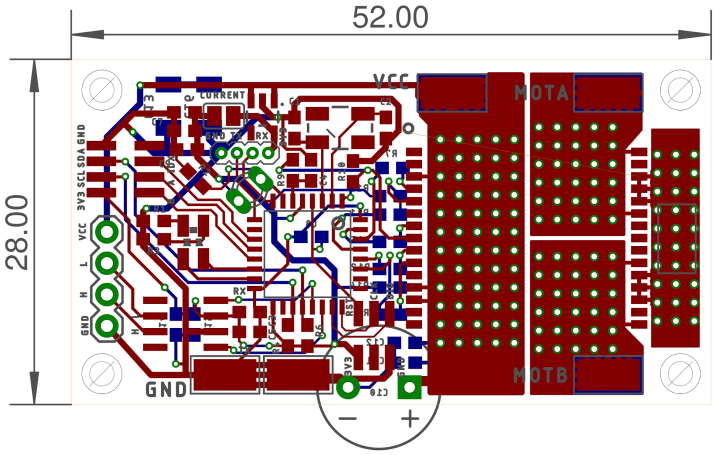

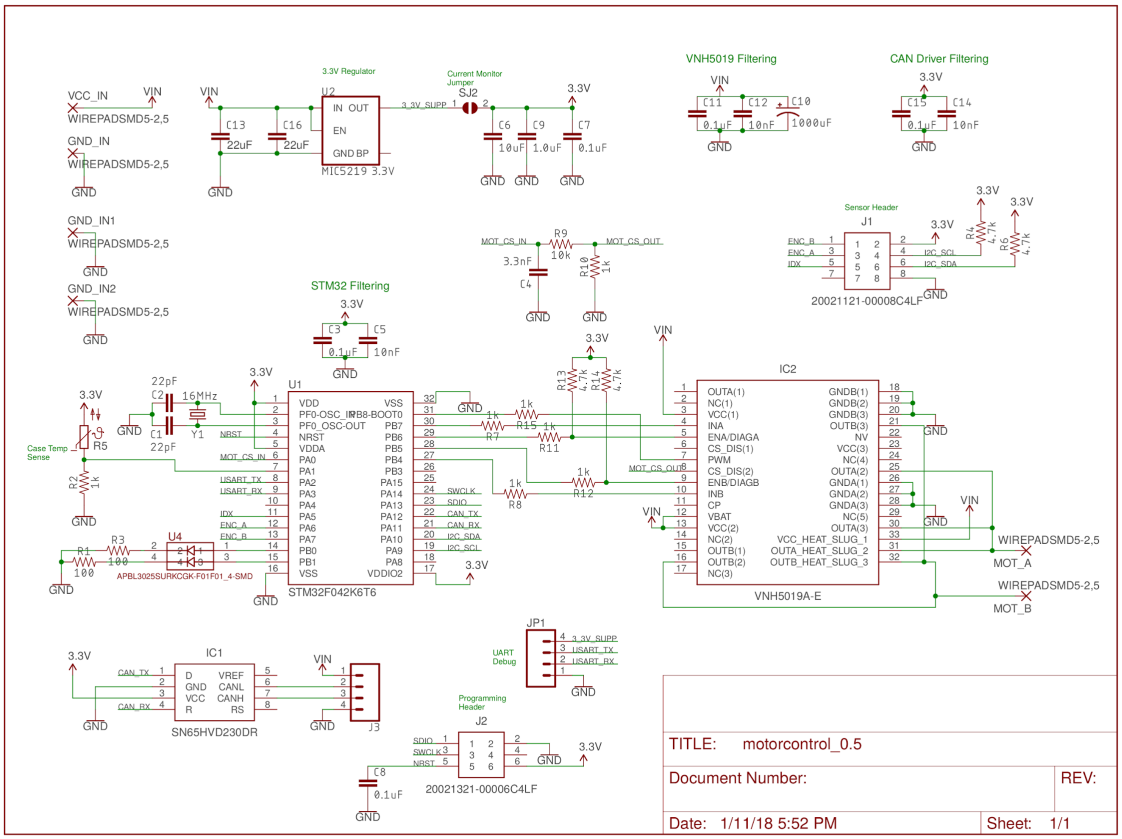

E Servo PCB Design

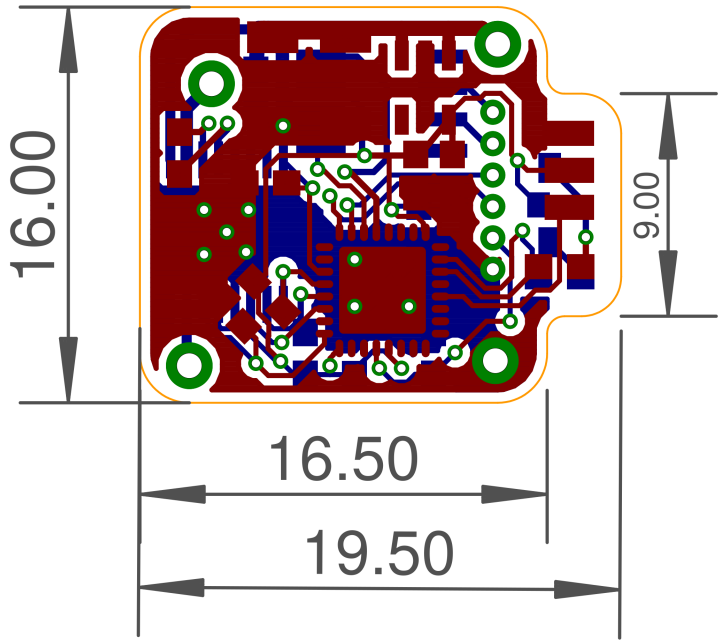

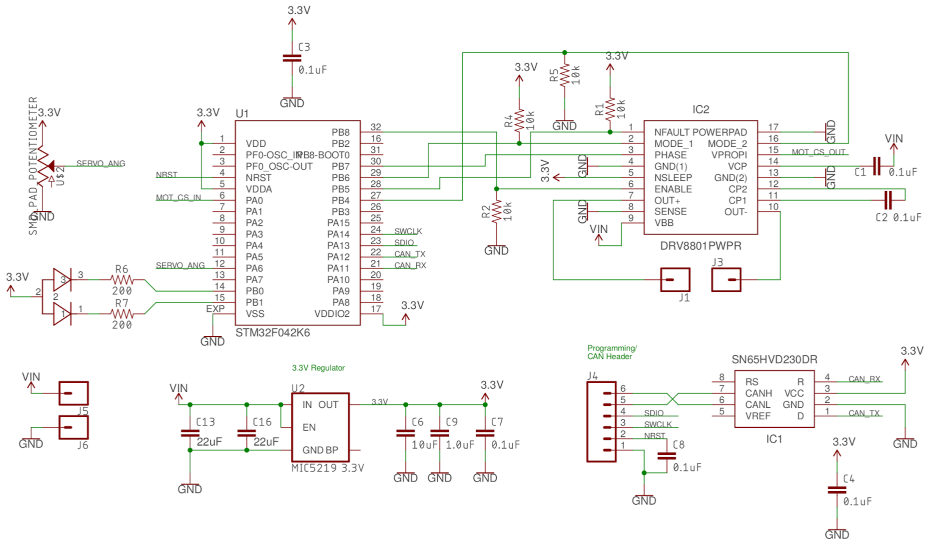

F Video Storyboards

This section contains storyboards created as part of the development of the Sailbot video. These storyboards contain narration, hypothetical interview lines, and rudimentary graphics as an outline for the final video.

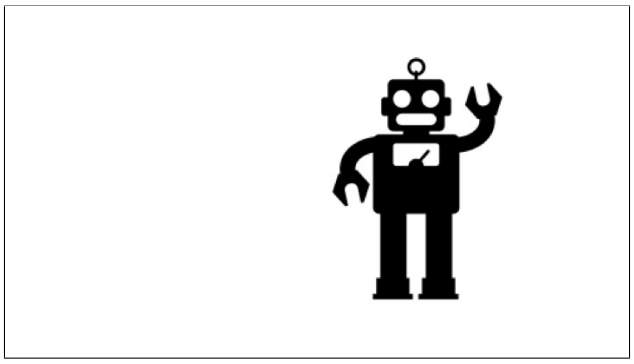

"What is a robot? Robots are often pictured as human-like machines with arms, legs, and heads, that are built to interact and inhabit the same world as humans." 0:09

"In pop-culture, they are often portrayed as humanoids" 0:04

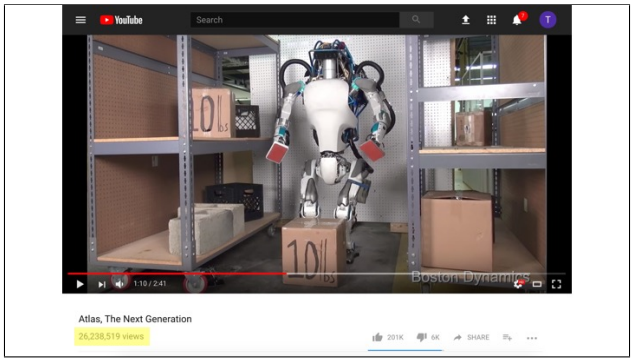

"and popular technology news often features humanoid robots accomplishing impressive feats." 0:05

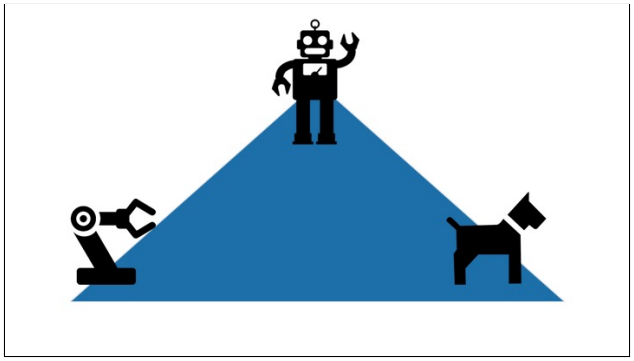

”However, the field of robotics extends far beyond humanoids, and with a wide variety of applications and appearances” 0:07

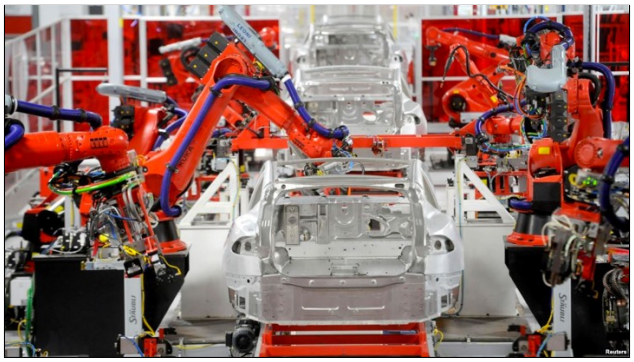

”In the manufacturing industry, large robotic arms perform various tasks from moving car bodies to painting and welding.” 0:08

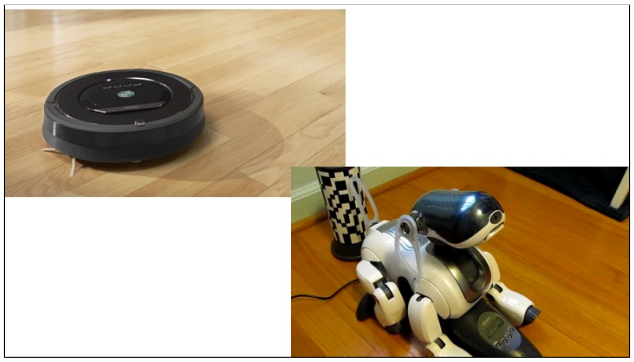

”In homes, robots that complete household chores and act as companions are becoming more common.” 0:08

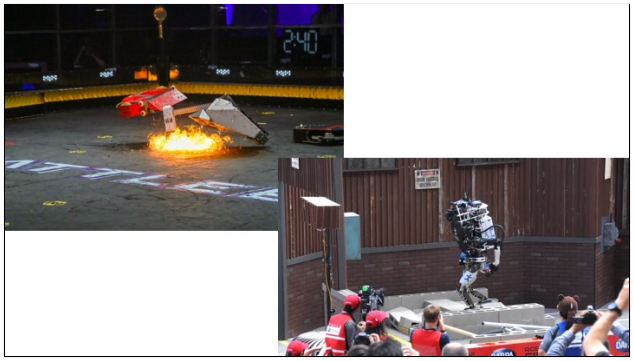

”Additionally, robots are often featured in competitions, whether for entertainment or advancing research in particular engineering fields. These competitions often feature teams from around the world” 0:10

”One of these robotics competitions is the International Robotics Sailing Competition. Teams from across the US and Canada design and manufacture sailboats to operate without any human action. These boats compete to complete different tasks, such as obstacle avoidance, station keeping, and endurance sailing.” 0:17

”In 2017, a team from Worcester Polytechnic Institute won the competition. Despite some technical difficulties, the team managed to perform very well in the competition. Their robot, called Sailbot, excelled in obstacle avoidance, endurance, and station keeping.” 0:15

"Sailbot is an autonomous sailboat designed to sail on lakes and oceans without any human intervention. It senses its GPS position as well as the windspeed. It uses this information to plan sailing manuvers to reach a goal, and then adjusts the sail and rudder accordingly. Sailing is a very complex task, and poses an interesting challenge for robotics engineers. TO EXPLORE THIS..." 0:20

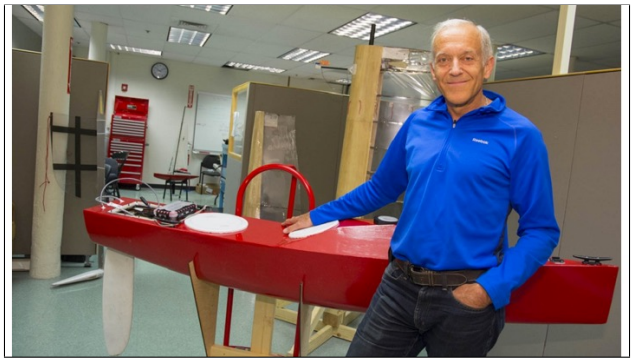

[Interviews with professors] 'The students did very well last year. We had a lot of success' 'It was great to see the success, and see how far it's come from when we started' 0:29

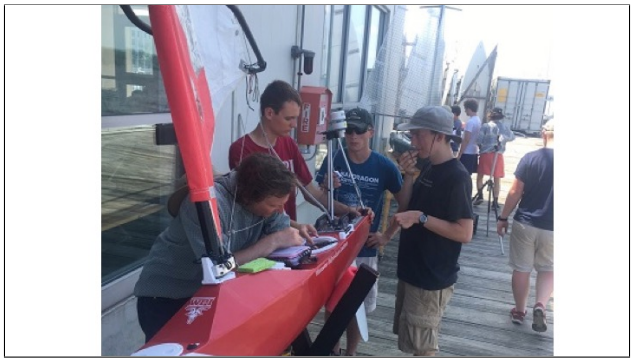

"Two of the team members, Jordan and Hans, started on the team as sophomores, and are currently working on the next version of Sailbot for their Senior year Major Qualifying Project." 0:10

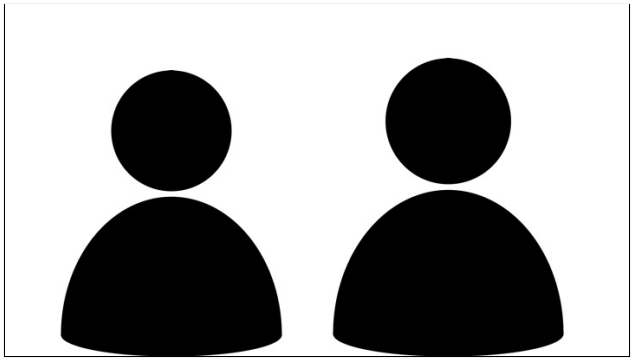

[Jordan and Hans talk about last year's competition] "It was a a lot of fun, and we did lots of cool things" "One of the biggest accomplishments was..." "One thing I think we can do a lot better is work on the control of the boat. There were some issues with how it sailed, as well as difficulty controlling the heel" 0:30

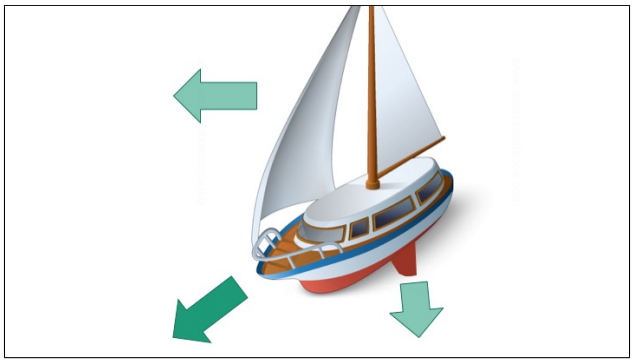

"What Jordan is talking about are two things, the balance of the boat from front to back, and the heel of the boat from side to side.

On a sailboat, there are actually two things that propel it forward. Above the water, the sail acts like a wing to push the boat forward and to the side. To counteract the sideways motion, below the water is what's called the keel that applies a force forward and across the other side. These sideways forces balance out, and the boat is able to sail forward. However, if the keel and the sail are not place correctly, these misaligned forces cause the boat to turn undesirably. It's like if you tried to ride a bicycle with the handlebars locked at an angle." 0:38

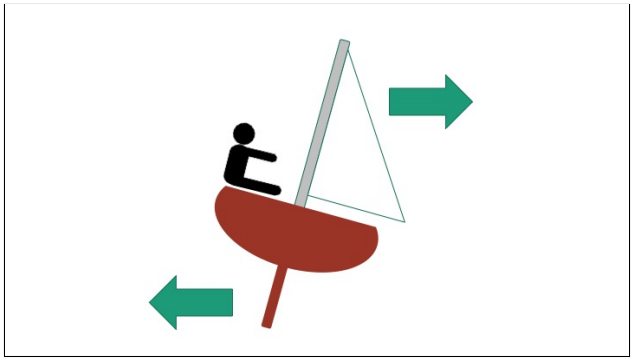

"The other challenge is controlling the heel of the boat, or how much it rolls from side to side. Since the sail and the keel produce forces in opposite directions, they naturally cause the boat to roll to the side. On

a traditional sailboat the crew compensates for this heel by leaning off the high side of the boat, and their weight helps the boat stay sailing. However, autonomous sailboats have no crew, so we need a different way of compensating for this force." 0:25

"This year, the team has been working to come up with solutions to this problem of control. " [Brainstorming discussion] "What if we tried a canting keel" "We could try something above deck instead" "Would that cause problems when it moves front-to-back" Etc. 0:20

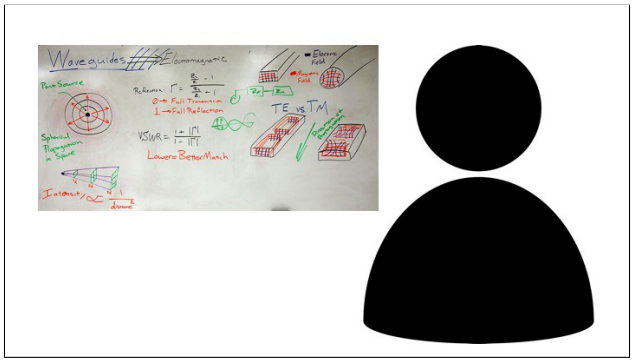

[Liam talking about the final solution] "So we looked at a couple different ideas and here's what we came up with. We are going to build a movable ballast system that can move a lead weight back and forth across the deck of the boat. It basically simulates the crew moving back and forth, and hopefully will give us the control we are looking for. 0:19

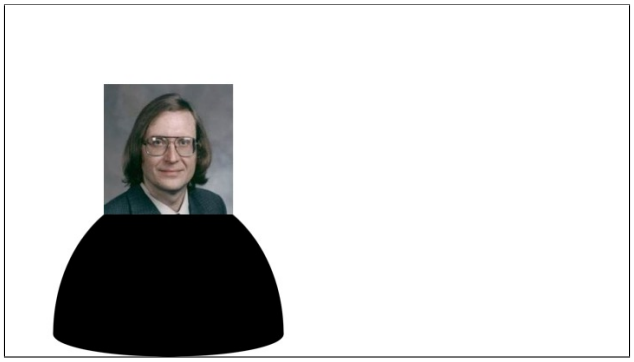

[Interview with professors]
"The movable ballast is a really innovative solution" "I think it will really add a lot to this robot" 0:20

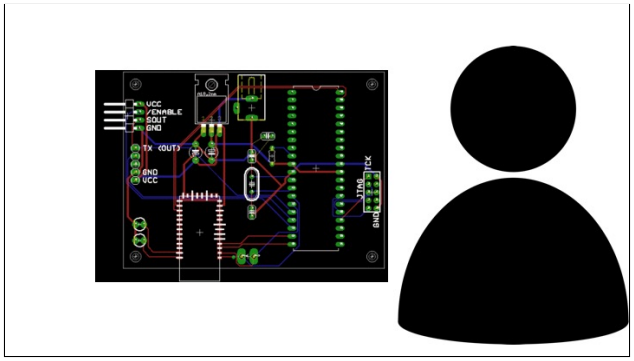

WITH THIS IN MIND, THE Team goes back to the drawing board. . . .

[Anyone] Another big challenge is waterproofing this whole system. Since it's going to be out on the water, we need to make sure that all of the electronics are safe and waterproof. That's why we are designing our own motor controllers using some standard marine electronics. While we are working on the mechanical assembly, we will also be working on these motor designs. 0:19

[Shots of manufacturing things]. 0:13

[Travis talking about problems]

So we ran into an issue. We planned to use this carbon fiber shaft for the arm, but it's much less rigid than we expected. There's also a lot of movement in the joints between the carbon fiber, so that causes a lot of bending in the arm as well. It's actually so bad, that we can't put the weight on without touching the deck. We are definitely going to need to redo these designs. 0:20

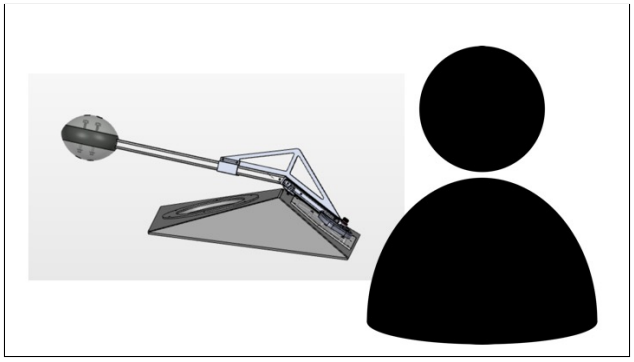

[Hans talking about designs]

"So instead of the carbon fiber links we used to have, we are now going to use a piece of machined aluminum. This will give us a lot more rigidity" 0:14

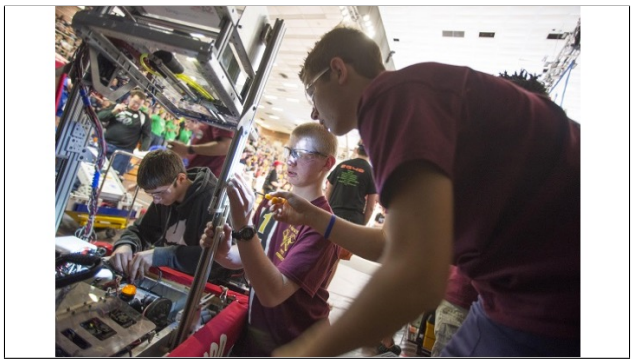

[Team assembling the arm]

"Well it fits now, that's a good sign" "Can we power it up and see how it does?" 0:08

"It works!" [shots of it working]

While there's still a lot of work that needs to go into Sailbot, a fully autonomous sailing system has plenty of applications 0:20

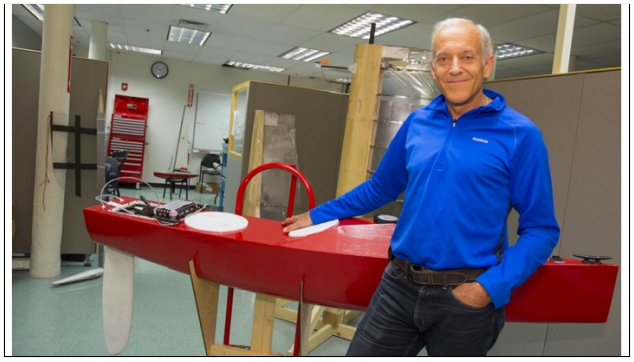

[Interview with advisors] “There’s plenty of applications for oceanic research...” “It could also be used in search and rescue...” 0:25

While sailbot is still in a research phase, it continues to explore new applications of robotics. While it may not appear to be anything special, this little boat is setting sail into uncharted waters. 0:12

G Video Testing Questions

User Testing Questions:

1. Which sections, if any, of the story were confusing?
2. Is there any part of the project you would like to know more about?
3. How likely are you to recommend this video to a friend?
4. What part of the story did you find most interesting?

Focus Group Questions:

1. What did you like about the video? dislike?
2. What was the main message of the video?
3. What did you learn from the video?
4. What was difficult to understand from the video?
5. Was there any parts of the video that you found boring?
6. Was there something missing from the video?